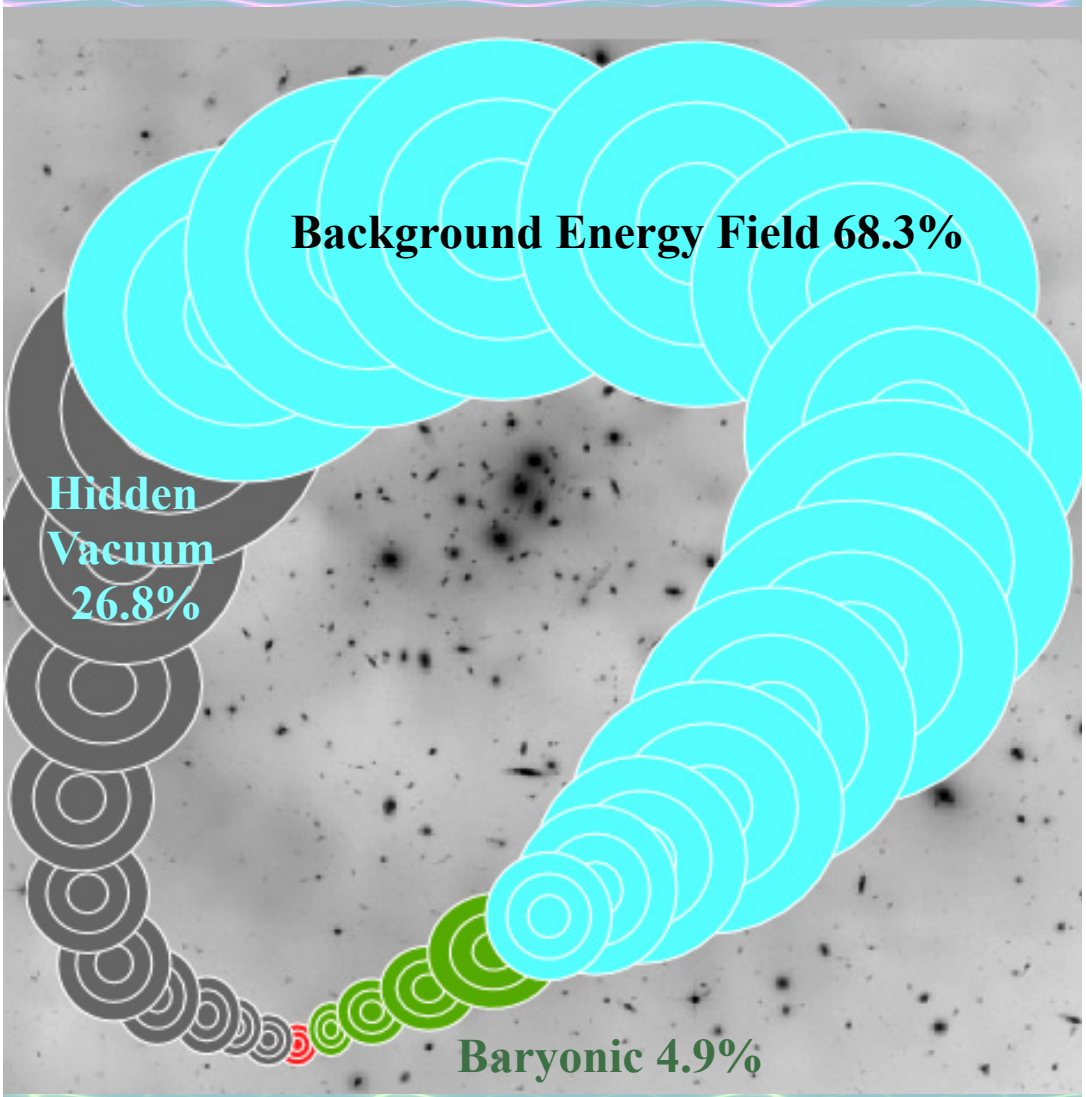

The Puzzle of Planck Mission

HUBBLE-INDEPENDENT PROCEDURE CALCULATING DISTANCES TO COSMOLOGICAL OBJECTS

J. E. Mullat *

Abstract. Our findings confirm Planck's satellite data on the composition of the Universe, based on which some predictions were made regarding the dynamics of the Universe in its past and future. On the same basis, a new procedure was developed for calculating distances to galaxies without the use of Hubble's constant. Then, the procedure for calculating distances was compared with the luminosity distances and the Hubble's law diagram, as well as with an alternative method for calculating distances linearly dependent on the redshift. Luminosity and Hubble's law distances for comparative analysis were found in the NASA/IPAC Extragalactic Database (NED), which is operated by the Jet Propulsion Laboratory, California Institute of Technology, under contract with the National Aeronautics and Space Administration. *"NASA/IPAC Extragalactic Database (NED) is a master list of extragalactic objects for which cross-identifications of names have been established, accurate positions and redshifts entered to the extent possible, and some basic data collected."* The results contradict rather than support the use of the Standard Cosmological Model.

Keywords: *Universe Composition; Quantum Vacuum; Red Shift; Visible/Baryonic Matter; Background Energy-Field*

1. INTRODUCTION

As far as the laws of mathematics refer to reality, they are not certain, and as far as they are certain, they do not refer to reality. Albert Einstein

The essence of this story is that our Universe could have formed from the gravitational—"background energy-field", which is considered as a qualitatively new form of matter. The gravity of the energy field is the fundamental basis of the world, generating vacuum voids and various anti-vacuum elementary baryonic particles. This leads to the fact that so-called gravitons continuously appear and disappear in it. If the strength of the gravitational field exceeds a certain level, gravitons can undergo a phase transition and turn into real particles.

From this point of view, the entire universe was filled with energy-field in a stationary but excited energy state, much higher than the current one. This state of matter is called *energy-field*, which has tremendous potential, but latent energy. As a result of a quantum leap, it

* *About the author*: Former docent at the Faculty of Economics, Tallinn Technical University, Estonia; Independent researcher. Docent is an Eastern European academic title equivalent to Associate Professor in the USA. Residence: Byvej 269, 2650 Hvidovre, Denmark, E-Mail: mjoosep@gmail.com.

passed into another, less excited state—*quantum vacuum*, then into baryonic matter, and then all of its energy was spent on the formation of the visible Universe. In this case, the quantum jump presumably comes from a strongly super-cooled symmetric phase below absolute zero. The result was an exponentially fast inflation of the universe. Before the quantum transition, the potential energy of the energy-field was incredibly high, but after that it turns out to be less.

During the quantum transition of the energy-field from one state to another the newly created space breaks simultaneously neither isotropically nor homogeneously up into quantum voids of vacuum and baryonic, i.e., visible matter in the form of quasars, galactic clusters, jets, flux, etc. The volume of the Universe becomes such that its distant parts turn out after inflation to be completely disconnected (Zeldovich et al., 1982), and each part of it will develop in its own way. Some will expand indefinitely, some will pulsate, some will contract and re-enter a state of high-energy; then restart new quantum transition again and generate new galaxies again. The newly created space in the inflation phase is very similar to the Big Bang, but it is not, because the newly created matter will be at rest but not in the state of an expanding ball.

Like raisins in dough, additional pockets of matter began to appear continuously in the dough, gradually layering the growing and created new dough. Simultaneously and in parallel in all the places around the Universe the energy loss of atoms in the dough were accelerated as the radius of the space filled with matter increased. We can thus assume that in space, as in a puff cake, the voids of the vacuum were gradually filled—the more vacuum was engaged in matter creation, the more energy from the outside came to the formation of new matter. The average energy density of the new space, however, decreased due to the loss of energy by atoms although the more energy as a whole was accumulated in due to the new space filled with matter.

The quantum transition of energy-field into matter can be explained by the assumption that first matter was formed with atomic distances inside the atoms of matter with a large extent. Electron's further from

the nucleus are held weaker by the nucleus, and thus can be removed by spending less energy. Thus, the dynamics of EM energy can be expressed using the formulas of quantum mechanics, assuming that the release of energy of atoms was initially small, and then the release of energy from atoms (atoms aged) gradually increased as new spatial voids layered. Consequently, light waves coming to us from the distant past should be shifted towards the red side of the visible spectrum.

It is also known that the primary heterogeneous in the *phase transition* of one form of matter to another sometimes lead to secondary heterogeneous in the secondary matter that is formed. Thus, we can then assume that, taking into account a contradictory, perhaps provocative hypothesis about the *gravitational transition* (Caldwell et al., 2005) of matter accompanying this transition by adopting a postulate of newly created particles of matter, which can be physically associated with different internal/intrinsic redshifts of areas of the same atoms that are formed simultaneously. The last statement, probably, justifies, Halton Arp (1966), assertion about the possibility of physical coexistence of cosmological objects with various redshifts in physical vicinity from each other inside so-called peculiar Arp's Galaxies.

As noted by Larry Abbott (1988), regarding Standard ΛCDM Model, cf. Bradley & Ostlie (2007) or Keel (2007), *"According to theory, the constant, which measures the energy of the vacuum, should be much greater than it is. An understanding of the disagreement could revolutionize fundamental physics"*. For the novel Γ-equation distance calculation, based on hypothesis of a gravitational transition of *energy-field* into *quantum vacuum* and *baryonic matter*, we use a similar Λ-constant, however, with only three parameters including Λ. In these somewhat novel terms of space dynamics in the Universe, we are comparing the Γ-equation calculations regarding the distances +over/–under estimates. In connection with this, the space-layering postulate is a fundamental element of the Γ-equation. We use the parameter μ of the average energy density of space, which must, by this assumption, constantly decrease.

One may wonder how the expanding postulate fits galaxies having the spectroscopic blue-shifted lines, such as the Andromeda galaxy. Is the light from Andromeda coming from the future? This paradox from the expanding perspective can be explained that astronomers cannot observe the effect of space expanding in neighboring galaxies. Instead, astronomers observe the relativistic Doppler effect, which dominates the expansion effect. This explanation of the redshift/blueshift indicates the dual nature, cf. Gupta (2018), of the parameter $1+z$. Most astronomers believe that Doppler effect is the correct answer, because they observe galaxies in the neighborhood. Few others rightly emphasize that the Doppler effect is not the correct answer, which has nothing to do with the reality, in particular when applied to cosmological objects located far away, thus having high cosmological redshift values.

Beyond a Reasonable Doubt, modern cosmology is undergoing a significant shift since many renowned scientists participate in revision of the general theory of relativity of space and time (Jones & Lambourne 2004; Copeland, Sami & Tsujikawa 2006; Gradenwitz 2018). The departure from the SM and the accepted view of the origin of Universe is driven by the realization that the theoretical predictions based on universal gravitation laws do not correspond to observations at a large scale, i.e., at cosmological distances and locations. The distant parts of the Universe, which we could observe on a large scale, for centuries, however, had, on average, a homogeneous and isotropic structure. Encoded in cosmology according to the Copernican principle, parameters such as energy density, brightness, etc. should be the same at all points and in all distant directions. The laws of gravity, provided that the Principle presumably corresponds to reality, will cause an unimpeded contraction of matter. In contrast, according to Adam Riess et al. (1998), Saul Perlmutter et al. (1999), gravity is not slowing down but actually speeding up the expansion with acceleration [i]. Indeed, many researchers are arguing that observations do not confirm the expansion (Lerner, Falomo & Scarpa 2014; Lerner 2018). Some others, including

J.G. von Brzeski (2018), are trying to disprove the expansion theory in general. While our goal is not to challenge conflicting or odious views, in this study we still look at the evolution of the universe from an *"expansion / growth"* perspective. In contrast to the SM, growth is postulated simultaneously with the disappearance of the *energy-field* regions due to the creation of a new static space, which, in turn, experiences a decrease in energy density. Our initiative shows that this growth of the newly created static space is manifested through the quantum vacuum as primary and baryonic matter as secondary, both of which pass through a gravitational transition from an unknown energy-field or ether, called also the zero point-field, quantum foam, gravitons, etc., into new space composition of growing three-dimensional spheres—manifolds S^3.

Hence, we hypothesize that a new space must emerge as soon as the space stable state has been established, since the old space composition violates the Γ-equation stable state criterion; cf. a) Mullat (1995), definition 2, p. 202. Based on this premise, the previous stable state violates itself, resulting in the creation of *"new space"*. This newly created space—a manifold in space—on average, as a whole, achieves a lower *"density of energy"* μ compared to that of the previous state. This violation arises due to such as latent *"gravitational energy forces"*, or any other energy form, induced into the manifold, providing a theoretical foundation for a stable states evolution as the dynamics of the Γ-equation roots. For this reason, in accord with the postulate of space layering, the declining density μ not only serves as an indicator of space creation, but also allows the time scale component of the space-time metric tensor—typically established by the t parameter—to be replaced by μ. While this is a far-reaching and highly unconventional assumption, it promotes a more diverse perspective on the dynamics of the space and energy evolution in the Universe. In view of the aforementioned assumption, the time variable in the time-space tensor will be omitted from all further considerations.

According to the NASA statement about the acceleration of visible Universe, for any alleged observer located at any point in the Universe and at any local time schedule in the past, the growth was slower than it is today. This statement by NASA invisibly hides the fact that the solutions of **Γ**-equation do not contradict NASA predictions about the dynamics of the universe in general. Yet, the math shows that Hubble constant is not a constant at all. In the past, perhaps, the value of Hubble constant was much lower than it is now, and it will be increasing in future. The question arises: what astronomers call dark matter (hereinafter—the quantum vacuum or something else—vacuum or matter), explains the contradictory characteristic features of the dynamics of baryonic matter, does such a Hubble constant refer to a quantum vacuum? Making this supposition, we found that, in the death phase, when the energy-field of the Universe will be almost exhausted, the dynamics of quantum vacuum in terms of *Vacuum Hubble Constant* will change its nature—the acceleration of the quantum vacuum area size will slow down. In contrast, the baryonic matter will still continue to expand its occupied area with acceleration by growing as usual the area extent and dimension with acceleration, like a window or bubble amid energy-field.

It was simple, to calibrate the **Γ**-equation of quantum vacuum and baryonic matter, as well as energy-field composition manifested by the equation, in order to match the 2013 Plank Mission satellite data. By solving the **Γ**-equation, it was possible to achieve 100% of exact co-occurrence between the obtained percentages of baryonic matter and quantum vacuum (dark matter) in their proportions to the background energy field and the latest data (Ade et al. 2013; Francis 2013; Clavin 2015). Second, our space/energy gravitational transition model supported the BB inflation phase. Theoretical foundations show that solely the quantum vacuum, cf. Tentanen 2019, first inflated three-

dimensional manifolds S^3 embedded in the globe $\Re^4$. Third, it is predicted that, after the inflation phase, as the manifolds S^3 expanded, its average energy density μ decreased, while volume-growth accelerated. This prediction was supported by the Γ-equation, the roots of which confirm that the manifolds initially expanded more slowly when the energy density was high.

Drawing upon the study pertaining to average density of energy parameter μ, it was possible to subject NED distances to a series of linear and non-linear transformation into a certain interval of densities. This interval confirmed with very high degree of reliability that it is feasible to describe the events in space with density μ by establishing a match to a number of distances to extragalactic objects collected in NED database[1]. We further posited a critical value κ of the density at which the gravitational/energy-field will be exhausted. We denote this event as the origin of density scale, i.e., the *"moment"* when the globe $\Re^4$ would allegedly collapse into *"standstill"* composition with critical density state. The Standard cosmological Model also supports a very high likelihood of such an event. We also confirmed some of NASA statements regarding the past evolution of the Universe.

Before we proceed with our analysis, we wish to outline the structure of this study, which is presented in 8 sections, including introduction—Section I. The section II might be helpful for understanding the mathematical foundation of our technique. In Section III, we present plausible/preliminary exercises by describing hypothetical energy-field undergoing a gravitational transition into quantum vacuum and baryonic matter on the basis of our geometric model. Applying initially the postulate of the gravitational transition of energy-field at distances almost equal to the Planck wall, in Section IV, the growth of space further on is a consequence of the postulate that is associated with a triplet of real parameters Λ, λ and μ in the form of a Γ-equation. We proceed further in Section IV dedicating our efforts to the energy density scale con-

[1] https://ned.ipac.caltech.edu/classic/forms/byname.html (accessed 29.06.2018).

struction, which is achieved by fine-tuning or calibrating latter triplet with regard to the current mass-energy composition of the Universe. In section V—the results—we consolidate the roots of the **Γ**-equation with the data pertaining to cosmological observations of 15000 Extraterrestrial objects collected into **NED** data[2]. Table 2-4 and Figure 5 present the data analysis summary. After the discussion in section VI, we provide some concluding remarks in Section VII. In Section VIII, we present mathematical derivation of three-dimensional series of manifolds S^3, which, in accordance with our initial hypothesis, are inflated with space. We illustrate in the Appendix the gravitational transition of energy-field by presenting our stereographical projection of the series S^3 of manifolds into Euclidian static space E^3. It should be noted that our model confirms rather than disproves the NASA statements of Universe dynamics, which are based on the past and current observations.

In conclusion, we should note that part of the material in our study, including Figure 1, as well as all the conclusions in the Appendix that led to our theoretical **Γ**-equation including our own mathematical derivation, which according to the result corresponds exactly to the metric of space, not so well-known in the literature (§108, p.336, *"Classical Theory of the Field"*, Landau & Lifshitz 1971, English edition), have already been published in the public domain, b) Mullat (1971).

2. Preliminaries

Suppose we pointed our telescope toward some portion of three-dimensional sky on which we superimposed a grid cell. By analyzing the characteristics of the light ray reaching us, we would allegedly be able to estimate the *number* of photons, electrons, and all atoms of various types of matter, including galaxies, in those particular moments when the ray was emitted. Once the process is complete, we can focus the same telescope on some other part of the sky. Assuming that the Copernican Principle is true, we can expect to obtain similar results when observing parts of the Universe at the same distance from our

[2] Received the data with kind permission from Ian Steer.

observation point in any direction. Such *measurements* will be particularly useful when the observations made are incompatible with Newton's dynamics—i.e., the measurements made at cosmological distances. In this scenario, the key challenge is to compare the energy densities of space measured at nearby and faraway distances as indicators of the layering dynamics of space and matter in the Universe. This type of measurements at cosmological distances can allow events to be described by the average energy density μ using the reciprocal relationships of events on the energy density scale.

By analogy with the postulate of the aging of atoms, it would be instructive to make the following remark from the bartender standpoint. We often see a sheet of paper burn out. If you start burning the sheet somewhere in the center, you will see that the front of fire will gradually spread out from the center, covering new areas, turning these areas into ash. By observing the combustion process somewhere inside the ash, it will be possible to measure the temperature of the gradually cooling ash and, on the basis of this measurement, determine how far away from the observer certain cells of the ash are.

Yet another bartender remark is also useful. Indeed, on Earth nuclear physicists can similarly determine the age of a material by noting the average number of atoms that have undergone radioactive decay. Using this approach, geologists can establish the age of a rock by observing unstable atoms undergoing a decay, recording the half of the atoms still present in the rock and comparing samples that have undergone the decay—referred to as radioactive half-life. Let us assume that we are able to count not only the average number of atoms undergoing the decay, but establish an exact number of atoms belonging, for example, to an Sn isotope in a rock. Let us further assume that we can do so with a high accuracy by taking into account every single atom remaining after the decay. Clearly, we cannot perform such an experiment. However, we can establish the *quasi-number* of atoms remaining after the decay as some *quasi-events* equivalent to the age of the rock under observation. By examining different parameters characterizing the rock, such as size, temperature, etc. We can establish the *quasi-velocity* of

these parameters by noting the number of atoms that have not yet undergone decay. In the same vein, we can establish the *quasi-events* in the Universe without recourse to the clock.

Returning to the earlier discussion on the observation of different parts of the Universe, we can also assume that the energy density μ of various particles (photons, electrons, neutrinos, galaxies, etc.) established through the observation of a nearby grid cell differs from that taken at faraway distances. We can now assert that, at nearby distances, the density in the grid cell is lower than that in the same cell when superimposed on parts of the Universe at faraway distances, representing their state at some point in the past. This assumption is in line with the Hubble's law rather than it contradicts the law. Thus, we can detect the age dynamics of the Universe using *energy densities* in these two locations, since regions with lower energy density (at nearby distances) have emerged during later events than similar areas characterized by greater density (at far away distances). Consequently, our aim is to emphasize that the energy density μ of energy can be chosen as an indicator of events in static space. Such an approach permits establishing the origin of time, whereby the density denotes time point $t = 0$ by $\mu >> 0$. Similarly, it will be possible to establish the future and the past on this scale, thus investigating the evolution of the Universe in terms of *energy density* instead of events on time scale.

Matter exists in four fundamental states—solid, liquid, gas and plasma—and can undergo a phase transition from one state to another. At normal atmospheric pressure, water is in solid state (ice) at temperatures below $0^\circ C$, whereby the liquid state symmetry transforms into crystal symmetry. In this context, it is noteworthy that a liquid can be cooled below its freezing point (known as super-cooling) without it becoming solid. Thus, when undergoing a phase transition to ice, water cooled below $0^\circ C$ can release latent heat (Murphy & Koop 2005). The same concept can be applied to gravitational energy, or whatever it is, as *"matter"* super-cooled under absolute zero ($0^\circ K$). This line of reasoning might prompt the conclusion that, in the Universe, a gravitational

transition of super-cooled *"gravitational field"* into space occurred, releasing an extensive amount of latent heat. The space released by transition expands; however, elsewhere at the globe surface, a latent *gravitational/energy-field transition* might take place simultaneously.

Three-dimensional coordinates can be used to measure the ice floe linearly. Yet, the volume of water is usually expressed in liters, rather than in cubic meters, etc. Speaking, for *Creatures* in the form of ice crystals, the water undergoing a phase transition is supposedly invisible, as they can neither observe nor measure phenomena pertaining to liquid matter. They can, however, feel the latent heat or space creation effects. From the mathematical perspective, the quantum vacuum, the gravitational, or whatever energy form we choose to consider, the energy can undergo a gravitational transition from zero to a positive measure state. Being rooted in the theory of Probability, measure is a means of assigning a numerical value to every space volume that allows examining the union of volumes as a sum of their individual measures. The space or mass of matter is an example of such a measure.

In contemporary cosmology, as previously noted, the Universe do not correspond to Copernican Principle of a homogenous and isotropic space presumably characterized by uniform distribution of galaxies at each point and in all directions, etc. The Principle, however, acknowledges the universality of laws of physics. These laws are applicable in the Universe with the same precision because there is no point of reference (although any point within the Universe could be used for this purpose). It is correct to recall a two-dimensional surface for flat *Creatures*, like that chosen by Einstein (1916), implying that flat *Creatures* cannot imagine a three-dimensional world by walking on the flat surface of a manifold. This analogy seemingly suggests that we as three-dimensional *Creatures "inhabit"* a three-dimensional static space. In this space, we are still observing a three-dimensional unbounded Euclidian space E^3, being inside of a bounded manifold $S^3(r)$ of radius r, $0 \le r \le 1$, embedded into four-dimensional closed hyper-globe $\mathfrak{R}^4$ of curvature radius 1. All manifold points, idealizing the Copernican Principle, are equal in all directions, without a center or a terminal point.

However, our view also accounts for departures (as shown in Zeldovich, Einasto, & Shandarin 1982) from the Principle, which as an absolute can never be realized in nature. Indeed, it is well known as already noted the primary anomalies in material undergoing phase or gravitational transition might result in secondary anomalies following the transition phase.

In the theory of choice, topology and some branches of social science, the emphasis is being made on the so-called Closer Operator, Pfaltz (2015). In this study, the closer operator is represented by constant Λ in Γ-equation to ensure new space creation dynamic. The constant Λ indicates the similar fixed-point stability of layering manifolds S^3, representing potential level Λ of the expected gravitational transition of the manifestation of energy-field. It seems that the Closer Operator mathematics introduces a novel idea in explaining the origin of the Universe.

To be more specific, our three-dimensional manifold of curvature radius $R = 1$—we prefer to denote it as a closed topology, i.e., a manifold S^3—comprises of a kind of energy-field that is not accessible to existing measuring instruments (akin to the *crystal creatures* not being able to use liquid measuring system in their solid world). As a result of some accident, at a given point within S^3, occurs energy-field gravitational transition into a seed lump of another form of space, which represents a transition of a 0-measure to a positive one. We emphasize that the lump of space formed from potential energy-field embedding the lump must preserve the stable or fixed point dynamic while undergoing rapid inflation from zero and progressing further, *like a hole growth* within energy-field similar to the discussions presented by Linde (1983a, 1984b). In short, the lump of space has to be in a dynamic Γ-equation with energy-field. The Γ-equation view on space dynamics is an alternative to SM, where the manifold curvature radius $R >> 0$ is time-dependent. In contrast, the curvature $R = 1$ considered here is constant. By making this assumption, we do not violate any mathematical foundations and do not try to dispute the postulates of rational science. Our goal is an alternative to the SM in order to give a reasonable interpretation of the paradoxes of astronomical observations.

The space creation singularity problem—the initial inflation phase, Guth (1997), of the Big Bang—has not yet been addressed. We argue that the singularity does not exist because our Γ-equation permits a zero solution. We thus postulate that, starting from a state described by the zero solution, the space suddenly inflates the infinitesimally small hole by seed of quantum vacuum in gravitational transition into static space from the aforementioned energy-field. The seed size might be not more of a size of a Planck wall. According to this view, when a *"lump of space"* emerges, it will impose an additional pressure on the previously allegedly *"super cooled gravitational energy"*, thereby causing an additional *inflating effect*. We further assume that this would give rise to additional space creation, akin to an *"avalanche"* rolling down the hill and gaining mass (and thus weight) due to *"potential gravitational energy of super-cooled energy-field."* According to our Γ-equation, the avalanche of the space creation has to remain in a dynamically stable condition. This assumption confirms that the gravitational transition of energy-field into quantum vacuum starts suddenly and will continue to progress if the *super-cooled energy* is of incredibly high energy density. After all, once the avalanche has occurred, it will govern the space creation inside the manifold. However, a *friable globe* cannot roll down a slope forever, as it would eventually crumble into pieces. While the *snow-globe dynamic* is just a bartender-physics illustration of the space evolution, it is useful for depicting its initial and terminal state.

3. The Model

In the continuation of our narrative, we combine some points to talk about the essence of the gravitational transition model in our understanding. Apparently, the reader could more smoothly follow our cosmological apparatus, which prompted us to more accurately disclose details that may remain intellectual speculations unless something similar does not reveal itself as a reality. In science, it is important, in which direction to move, so as not to be at an impasse. Mathematically, everything is in order here, since we will have rich computational capabilities and will be able to formulate a sufficient number of non-trivial predictions.

3.1. Pedagogical preface.

Consider a field W of high-energy environment consisting of 5 items $W = \{\alpha_1, \alpha_2, ..., \alpha_5\}$ or gravitons. There is no need to refer to these main ingredients $W = \{-5, -1, -1, -5, -1\}$ in any other way than, for example, to cells, particles, etc. Negative numbers conceal a latent energy below absolute zero or status of cells indicating that the high energy-field gravitational transition of the cells into space is potentially available. Positive values will indicate the fact of the gravitational transition into matter. Using these 5 cells, one can arrange subsets or compositions of cells where the process of transition completed, for example, 4 of which will be $X_{5,1} = \{5,1\}$, $X_{1,1,5} = \{1,1,5\}$, $X_1 = \{1\}$, $X_{5,5} = \{5,5\}$, etc. So, $|X_{5,1}| = 2$, in $|X_{1,1,5}| = 3$, $|X_1| = 1$, $|X_{5,5}| = 2$ point at digits of gravitons. Let's talk about, e.g., some high-energy indicators $\pi(\alpha, X) = \alpha \cdot |X|^{-1}$ of the gravitational transition into space cells. Numerical values $\pi(\alpha, X)$ are defined within indicated subsets X of cells. The negative index $u = \pi(\alpha, X)$, as a parameter in the form of threshold u may indicate enormous energy level when the latent energy is turning into positive value by supposition. In particular, $u = -\frac{1}{3}$ will indicate soon some phase transition constant, e.g., gravitational potential force or pressure, temperature threshold etc. Negative index points that transition is impossible but latent. Positive values will point at inverse situation – transition is potentially available. So, the potential gravitational transitions events with our high-energy cells may arrange the following lists:

$$\{\pi(\alpha, X_{5,1}\} = \{-\tfrac{5}{2}, -\tfrac{1}{2}\}, \{\pi(\alpha, X_{1,1,5}\} = \{-\tfrac{1}{3}, -\tfrac{1}{3}, -\tfrac{5}{3}\},$$
$$\{\pi(\alpha, X_1\} = \{-\tfrac{1}{1}\}, \quad \{\pi(\alpha, X_{5,5}\} = \{-\tfrac{5}{2}, -\tfrac{5}{2}\}.$$

Given a list $\{\pi(\alpha, X)\}$, we consider the value $F(X) = \min_{\alpha \in X} \pi(\alpha, X)$ on each X. Turns out that $F(X_{5,1}) = -\frac{5}{2}$, $F(X_{1,1,5}) = -\frac{5}{3}$, $F(X_1) = -\frac{1}{1}$, $F(X_{5,5}) = -\frac{5}{2}$. In standard notation we can consider a kernel subset X^*, which satisfy a condition: $X^* = \arg\max_{X \subset W} F(X)$, where the subset X^* deliver the function $F(X)$ global maximum – the **min/max** problem.

Until now we have considered only 4 compositions. What if we look at a space bubble W or sphere of cells in the form of a 3-dimentional room, which e.g., consists of a 10^{215} cells. Then the number of gravitational transition subsets $X \subseteq W$ under consideration will be equal to $2^{10^{215}}$. Now our task at first glance will be *mission impossible* to find a kernel among all such a subsets on which the minimum of the function $F(X)$ is reached. However, the problem is solved simply.

Let us illustrate the solution on the example of our 5 cells $W = \{-5, -1, -1, -5, -1\}$. First, we need to arrange the cells $W = \{-5, -1, -1, -5, -1\}$ in descending order of α-numbers in brackets in the form $\langle W \rangle = \langle -1, -1, -1, -5, -5 \rangle$. Then we will move along $\langle W \rangle$ from the left to right, examining the cells while moving along the arranged list of compositions $X_1, X_{1,1}, X_{1,1,1}, X_{1,1,1,5}, X_{1,1,1,5,5}$. We attach the cells one by one to each composition in the sequence, keeping in mind that the attached cell is undergoing a phase transition, until we fill in the whole composition $\langle W \rangle$. Consequentially, while moving to the right, the potential (or latent) gravitation energy indicators $F(X_1), F(X_{1,1}), F(X_{1,1,1}), F(X_{1,1,1,5}), F(X_{1,1,1,5,5})$ corresponding to the sequence $\langle -\frac{1}{1}, -\frac{1}{2}, -\frac{1}{3}, -\frac{5}{4}, -\frac{5}{5} \rangle$ are considered. The local maximum $u = -\frac{1}{3}$ is reached on the composition $X_{1,1,1}$, which is the solution to our problem of phase transition among all the 32 compositions. As promised, it is obvious now that an exactly the same algorithm among all the compositions in the bubble W of the size equal to $2^{10^{215}}$ works *"perfectly."*

Without prejudice to what has been said, looking ahead, we would like to note that in our cosmological model reg. distances calculations to galaxies there are similar functions $\{-\pi(\alpha, X)\}$, i.e., functions that increase (as negative) in accord of X growth: for example, the function of Newtonian gravitational potential function $-G\dfrac{M}{r(X)}$. The X is an interior set while $\overline{X}$ is the outside set: $X \cup \overline{X} = W$, $r(X)$ denotes the radius

of X. The kernel X^* in our pedagogical nomenclature will then be, once again, where the function $F(X) = \max_{\alpha \in X} \pi(\alpha, X)$ reaches its maximum, cf., Mullat 1971.

3.2. General considerations

So, let a certain field (e.g. Gravitational energy-field) W be given in which the field folds can pass from one state to another. It does not make a difference at first what these states are. It is important that there are two states, two phases from which the high-energy cells W are folded. Each cell can be in two states—matter and energy, i.e., the cells can transit from the energy to matter and back.

Since this view on the field W is taken for something real or reasonable, it is very natural to consider the set 2^W of all subsets or high-energy cells W in which the gravitational transition can happen, and let them be subsets of cells acting as cells compositions $X \in 2^W$, $X \subseteq W$. Such an abstraction in the notation represents the most common standard in set theory.

However, not being an experienced high-energy physicist and having no idea how a high-energy gravitational transition takes place, it can still be assumed that all cells $x \in X$ represent a potential transition from latent gravitational energy states to a materialized state, while all those cells $\overline{x} \in \overline{X}$ that are in a state of potential transition as some candidates are only labeled as such. The set $\overline{X}$ is the part of W unfilled by cells from X. Shortly speaking $X \cup \overline{X} = W$ or $\overline{X} = W \setminus X$.

Now we need to say a few words about what we are going to consider for the compositions of cells X. In theory of measure we consider some *"good"* subsets of cells that can be measured: such as having mass measured by weight in kg^1, volumes in m^3 or liquids in lt^1 or galloons of gas, energy density in j_s per kg, etc. The starting point of the theory of measure is the probability theory. We not accidentally talking about probability, since it is very natural to link the high-energy gravitational transition of any cell $\alpha \in W$ with the certain *"quantum probability"*

$\pi(\alpha, X)$ that the gravitational transition will occur as a subject of the transition itself. Note that the probability estimates $\pi(\alpha, X)$ may be defined on W but inside X. That is, we consider a set or a family of parametric functions $\{\pi(\alpha, X) : X \subseteq W\}$ consisting of $2^{|W|}$ individual functions dependent on a parameter X in the form of a subset of cells in the aggregated high-energy medium of measurable cells W. It is possible that some kind of quantum effects can play a role here, since this is about probability.

Now, we reached the most important point. Suppose that in the aggregated high-energy-field W the cells are characterized by a certain distribution functions $f(\alpha)$, $\alpha \in W$, or whatever we want to interpret these functions. These functions may be some initial force acting in the cell α like temperature, pressure, etc. We cannot imagine or say more, but the following phenomenon is important. For example, we can associate this function with some estimate (not with the probability but a gravitational transition process itself), for example, by setting $\pi(\alpha, X) = \frac{f(\alpha)}{|X|}$, where $|X|$ it is weight, volume, etc., which aggregate cells X. We can also supposedly associate this function with some threshold u when the gravitational transition occurs. Such functions can be constructed in order to satisfy many conditions but one mandatory condition, which is characterized by the so-called monotonicity property. Indeed, suppose we consider two subsets of cells L, G such that $L \subseteq G$, then the following monotonicity property should hold: $\pi(\alpha, L) \le \pi(\alpha, G)$ for all $\alpha \in L$.

Finally, we meet the main assumption. Based on the proposed scheme for any set of cells $X \subseteq W$, we have a certain probability function on the anti-gravitons $\bar{x} \notin X$ that are outside X of the indicated by using the function $\pi(\bar{x}, X)$ of the probability of a gravitational transition in an outside cell $\bar{x}$. Suppose that the gravitational transition is determined by a certain threshold value u of the function $\pi(\bar{x}, X)$, namely: in the set X the gravitational transition can take place only if $\pi(x, X) \ge u$, while for $\bar{x}$ out of X, it can be $\pi(\bar{x}, X) \ge u$ either

$\pi(\bar{x}, X) \le u$, in the latter case the transition cannot take place. A similar view on gravitational transitions gives rise to the display of subsets in two equivalent aggregate compositions of cells W:

$$V_u(X) = \{\alpha \in W | \pi(\alpha, X) \ge u\}, \text{ or } V_u(X) = \{\alpha \in W | -\pi(\alpha, X) \le -u\}.$$

In theories, speaking of mappings, we always are interested in the so-called fixed points, (i.e., fixed point theorem of Brauwer). In our case, we will also be interested in fixed points of mapping $V(X)$, i.e., such subsets X of cells of the field:

$$V_u(X) = X. \Leftarrow \mathbf{\Gamma}\text{-equation}$$

Given a sequence $X_0, X_1, ... X_i, ...$ such that $V_u(X) = \lim_{i \to \infty} X_i$, $X = X_0$. $X_0 \subset X_1 \subset, ...$ it is simple to figure out what these fixed points $V_u(X)$ of mappings are. Perhaps $V_u(X)$ is a state of space or the high-energy state of the field when the phase or gravitational transition process stopped, etc. We claim that **Γ**-equation in our cosmological model devoted to distances calculation to galaxies corresponds to a fixed point in terms we just have been described. For some researches this terminology in choice theory represents so called closer operator $V_u(X)$ performed on X.

3.3. Summary

The fairy tale that we have just told is irrelevant to reality, but it can become one if we can formulate what a high level energy-field W might be, for example, it could be a cylinder, a globe, a surface of a globe, etc. In our findings calculating of the distances to galaxies we were able to define the field W as a stereographic projection of the diverse surface $\boldsymbol{S^3}$ of the globe $\boldsymbol{\mathcal{R}^4}$. Functions $\pi(\alpha, X)$ were chosen as the potential energy $-\frac{G \cdot \mathcal{E}}{c^2 \cdot \rho^\lambda} = -\frac{\mathcal{E}_{rel}}{\rho^\lambda}$ like the gravitational potential, where the radius ρ of the Universe was given in terms of the stereographic projection of Landay-Lifshitz metric space, which is actually the Euclidean space E^3. A separate element outside our visible Universe can be interpreted as an element of energy-field, undergoing a potential

gravitational transition into atoms, or whatever high level energy baryonic particle like leptons, neutrinos, etc., when the high energy cell undergoes a gravitational transition into cells α of baryonic matter. The parameter threshold u at which the gravitational transition presumably occurs is set to a constant Λ. However, above, until now, the parameter was defined as a variable u. This contradiction is simply solved by introducing an energy density μ parameter of the cell α. Now it's clear which parameter Λ or μ—the threshold parameter or the energy density parameter—should be a variable parameter and which should become a constant.

Of course, more natural is to set the energy density μ as a variable parameter leaving some constant value behind Λ. The μ parameter will make it possible to find the total energy $\mathcal{E}_{\text{rel}} = \mu \cdot \text{V}.\boldsymbol{S}^3(\rho)$ of the hyper-manifold $\boldsymbol{S}^3(\rho)$; mathematical derivation in the Appendix. This is an important decision, since it allows building an energy density scale μ using some extents of the redshift z. However, when performing simulations by trial and error with the NED database, it would be prudent to replace the μ parameter by a decay function $\mu \approx 1 - \left(\frac{1}{2}\right)^{Z}$.

4. The tale of the space creation

Our knowledge of the Universe is limited by the horizon of observations. This horizon is determined by the speed of light, whereby we can only observe those areas of the Universe from which the light has already reached us. Hence, we do not see the objects in their present state, but rather in the one in which they were at the time of the emission when the ray of light has reached us at the moment of observation. In view of the foregoing, it is assumed that the universe can be described in terms of some geometry, the main characteristic of which is the distance r to some point in the universe, regardless of whether the ray of light has reached the point or where the point is located.

The distant parts of the Universe, which we could observe on a large scale, for centuries, however, had, on average, a homogeneous and isotropic structure. Encoded in cosmology according to the Copernican

principle, parameters such as energy density, brightness, etc. should be the same at all points and in all distant directions. Assuming that the Copernican Principle is true, we can expect to obtain similar results when observing parts of the Universe at the same distance r from our observation point N in any direction.

4.1. Stereographical mapping

In crystallography, various projections are used for the spatial image of the crystals under study, their symmetry and limiting elements. The most commonly used is a gnomo-stereographic projection. The gnomon is a scientific instrument that can cast a shadow on a perpendicular plane to determine the declination of the sun throughout the year.

To construct a crystal projection, the latter is placed in the center of a spherical surface. The faces and edges of the crystal continue until they intersect with the spherical surface and are depicted as follows: the faces are in the form of arcs; the edges are in the form of points. This projection is called stereographic. For a more visual image of crystals, a gnomo-stereographic projection is used. In this case, it is not the face that is projected, but the perpendicular to it; the planes normal to them replace the projections of the edges. In gnomo-stereographic design, faces give points on a sphere, and edges — arcs.

We will work based on Occam's Razor (it has a history dating back to Aristotle) methodological principle of parsimony: *"You must not multiply things unnecessarily* or *You must not attract new entities unless absolutely necessary …"*, accessed online, 08.08.2021). In particular, we are trying to abandon any high-rank tensors, time coordinates, laws of gravity, etc., focusing only on the standard quadratic forms of differential geometry.

We will investigate the metric of space given by the form

$$dl^2 = \frac{dr^2}{1-\left(\frac{r}{a}\right)^2} + r^2 \cdot \left[\sin^2(\theta)\cdot d\varphi^2 + d\theta^2\right]. \tag{1}$$

The form (1) was considered in "Classical Field Theory", Landau-Lifshitz (LL), 3rd Revised English Edition, 1971, p. 336.

The metric depends on the curvature radius a, where the r can vary from 0 to a, and where φ and θ are in the intervals $[0 \le \varphi \le 2\pi]$ and $[0 \le \theta \le \pi]$. It turns out that the quadratic metric (1) can be considered as a stereographic projection of the surface $\mathcal{S}^3$ of the four-dimensional ball $\mathcal{R}^4$ onto the flat Euclidean space E^3. Indeed, as an exercise, the substitution $r = \dfrac{r_1}{1 + \dfrac{r_1^2}{4 \cdot a}}$ for $0 \le r_1 \le a$ lead to

$$dl^2 = \left(1 + \frac{r_1^2}{4 \cdot a^2}\right)^{-2} \cdot \left(dr_1^2 + r_1^2 \cdot d\theta^2 + r_1^2 \cdot \sin^2\theta \cdot d\varphi^2\right). \tag{2}$$

According to LL's idea, at each point of the three-dimensional manifold $\mathcal{S}^3$ the metric (1) would be locally Euclidean, but curved at large distances. The metric transformation, the mathematical derivation of which in section 4.3 after further substitution $r_1 = 2 \cdot a \cdot \rho$ for $a = 1$, will exactly match its stereographic metric form:

$$dl^2 = \frac{4}{\left(1 + \rho^2\right)^2}\left[d\rho^2 + \rho^2\left(\sin^2(\theta)d\varphi^2 + d\theta^2\right)\right]. \tag{3}$$

Moving $r = \dfrac{2 \cdot \rho}{1 + \rho^2}$ from $r = 0$ to 1 (hence moving $\rho = 0$ to 1), and then backwards moving $r = 1$ to 0 (hence moving $\rho = 1$ to ∞) it appears to be two bubbles inside the stereographic interval $[0 \le \rho = 1 < \infty)$. At this interval, these two bubbles are spaced along the boundary $\rho = 1$ in such a way that the bubbles overlap each other at every point at a distance r from the common Center$(0,0,0)$. The volume of each bubble is equal to π^2.

The reader can now check that the substitution of $r = \frac{2 \cdot \rho}{1+\rho^2}$ into the form (1) leads exactly to the same metric as (3) in accord to p.8 at the end of the division 4. This proves that the LL metric is nothing but a stereographic projection of the surface of the 4-dimensional manifold $\mathcal{R}^4$ into the Euclidean flat 3-x dimensional space E^3.

The article is divided into four Sections, excluding the introduction. First, in the Section 2, as an exercise, a stereographic mapping of a two-dimensional surface $\mathcal{S}^2$ of a three-dimensional ball $\mathcal{R}^3$ is given on a Euclidean plane E^2 perpendicular to the axis connecting the North Pole $N = (0,0,+1)$ with the South Pole $S = (0,0,-1)$ of the boll. Then, in Section 3, the same stereographic mapping is generalized to a four-dimensional manifold $\mathcal{R}^4$ where the three-dimensional surface $\mathcal{S}^3$ of our manifold $\mathcal{R}^4$ already becomes the image of the stereographic mapping, namely the three-dimensional Euclidean manifold E^3 perpendicular by analogy with the axis now connecting the North Pole $N = (0,0,0,+1)$ with the South Pole $S = (0,0,0,-1)$. In Section 4, the mathematical derivation of the Landau-Lifshitz metric space is given in the form of a stereographic projection.

In conclusion, we present the result of calculations on the partition of our three-dimensional Euclidean surface $\mathcal{S}^3$ of the manifold $\mathcal{R}^4$ into three regions exactly corresponding to the composition of visible and dark matter, and what cosmologists today call dark energy according to Planck missions satellite data for 2013: **4.9%** visible or baryonic matter, **26.8%** dark matter and finally **68.3%** dark energy.

4.2. Stereographical projection of two-dimensional surface

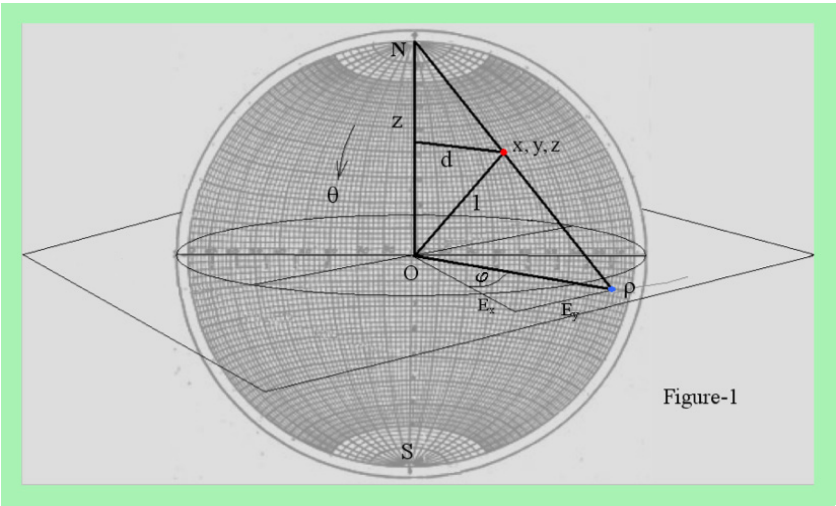

Figure 1: Surface $\boldsymbol{S^2}$ of the globe $\boldsymbol{\mathcal{R}^3}$ stereographical projection at Euclidian Plane E^2.

We will proceed first with a very short illustration of what is well known as stereographical projection. Let the $\boldsymbol{S^2}$ manifold geometry correspond to $x^2 + y^2 + z^2 = 1$ of curvature radius 1. The North Pole corresponds to the point $N = (0, 0, 1)$, and the South Pole is denoted by $S = (0, 0, -1)$. Conceive Euclidian plain E^2 intersecting the origin $O = (0, 0, 0)$ perpendicular to the z-axis. We can project a line from N through $(x, y, z) \in \boldsymbol{S^2}$, which will intersect the plain at a distance ρ from the origin O. Using $\boldsymbol{S^2}$ geometry it can be verified that $d^2 + z^2 = 1$ what yields $d^2 = (1 - z)(1 + z)$. Now convert $\frac{d}{\rho} = \frac{1 - z}{1}$ into $d^2 = \rho^2 (1 - z)^2$. For latter d^2's these d^2 yield $z = \frac{-1 + \rho^2}{1 + \rho^2}$, $d = \frac{2 \cdot \rho}{1 + \rho^2}$ what match up a stereographical projection, given by threefold projection/mapping $\left(\frac{2 \cdot \rho}{1 + \rho^2} \times \cos(\varphi); \frac{2 \cdot \rho}{1 + \rho^2} \times \sin(\varphi); \frac{-1 + \rho^2}{1 + \rho^2} \right)$ of two variable functions as a diffeomorphism $S^2 \to E^2$ into coordinates (E_x, E_y) on Euclidian plain E^2: $(E_x, E_y) = (\rho \cos(\varphi), \rho \sin(\varphi))$, $0 \le \varphi \le 2 \cdot \pi$, $0 \le \rho < \infty$.

Let us finally find the metric of our stereographical projection drawn by Figure 2. The partial derivatives of the projection/diffeomorphism represent the Jacobin matrix J. The transpose of the matrix J is thus given by three functions of two variables:

$$\mathrm{J}^{\mathrm{T}} = \left\| \begin{matrix} 2\cdot\dfrac{1-\rho^2}{\left(1+\rho^2\right)^2}\times\cos(\varphi); & 2\cdot\dfrac{1-\rho^2}{\left(1+\rho^2\right)^2}\times\sin(\varphi); & \dfrac{4\cdot\rho}{\left(1+\rho^2\right)^2} \\ -\dfrac{2\cdot\rho}{1+\rho^2}\times\sin(\varphi); & \dfrac{2\cdot\rho}{1+\rho^2}\times\cos(\varphi); & 0 \end{matrix} \right\|.$$

Consequently, the Gram Matrix as the static space metric tensor $\mathrm{G}_{\mathrm{i,j}} = \mathrm{J}^{\mathrm{T}} \times \mathrm{J}$ yields $\mathrm{G}_{\mathrm{i,j}} = \dfrac{4}{\left(1+\rho^2\right)^2}\begin{pmatrix} 1 & 0 \\ 0 & \rho^2 \end{pmatrix}$ provided by Скляренко (2008). Herby, our $\mathcal{S}^2$ stereographical projection on Figure 2 is represented by $\mathrm{dl}^2 = \dfrac{4}{\left(1+\rho^2\right)^2}\left(\mathrm{d}\rho^2 + \rho^2\mathrm{d}\varphi^2\right)$. We will refer later to substitution $\mathrm{r} = \dfrac{2\cdot\rho}{1+\rho^2}$ representing the *"inverse"* part of the diffeomorphism of $\mathcal{S}^2 \to \mathrm{E}^2$ or $\mathcal{S}^3 \to \mathrm{E}^3$ stereographic projections, where dl^2 denotes the metric in the Euclidian plain E^2. This means that it will be possible to refer to manifolds $\mathcal{S}^3(\mathrm{r}) \equiv \mathcal{S}^3\left(\dfrac{2\cdot\rho}{1+\rho^2}\right)$, which are now given as a function of ρ radius coordinate, and not of the radius r but as a projection radius ρ onto the Euclidean manifold, Figure 2.

4.3. Stereo-graphical projection of three-dimensional surface

Unfortunately only a few people can conceive a four-dimensional hyper-manifold $\mathcal{R}^4$. However, the aforementioned process can be applied to a $\mathcal{S}^3$-dimensional surface of the $\mathcal{R}^4$ dimensional globe. Around the North Pole $\mathrm{N} = (0,0,0,+1)$ as a reference system center, try

to envision drawing an imaginary $\mathcal{S}^3(r)$ manifold given by polar coordinates of radius r, $0 \le r \le 1$. Our $\mathcal{S}^3(r)$ manifold is of a fixed curvature of radius 1. Proceed in similar way already described above for an ordinary globe $\mathcal{R}^3$ encircling point N until the whole $\mathcal{S}^3$ surface of the $\mathcal{R}^4$ globe is inflated.

At cosmological distances, the space purported to be homogeneously inflated with space energy and matter and is completely isotropic. The generic metric that meets these conditions is given by S^3 manifold of four-dimensional globe $\Re^4$. In the derivation below, we will consider only the case of closed model with positive curvature ≈ 1.

$$x^2 + y^2 + z^2 + r^2 = 1$$
$$x^2 + y^2 + z^2 \le r^2 \le 1$$

These equations represent so-called closed space manifolds $\mathcal{S}^3(r)$ of curvature 1 on the surface enclosing four-dimensional hyper-globe $\mathcal{R}^4$

The spherical coordinates x, y, z are related to the E^3 coordinates by $\varphi = \tan^{-1}\left(\frac{y}{x}\right)$, $\theta = \cos^{-1}\left(\frac{z}{r}\right)$, where $r = \sqrt{x^2 + y^2 + z^2}$.

$$x = r \cdot \cos(\varphi) \cdot \sin(\theta),$$
$$y = r \cdot \sin(\varphi) \cdot \sin(\theta),$$
$$z = r \cdot \cos(\theta), \quad \text{where} \quad 0 \le r < 1,$$
$$0 \le \varphi \le 2 \cdot \pi, \text{ and } 0 \le \theta \le \pi,$$

The stereographical projection $\mathcal{S}^3$ from North Pole $(0, 0, 0, 1)$ intersecting $\mathcal{R}^4$ at the origin $O = (0, 0, 0, 0)$ perpendicular to line connecting North N with South Pole S is given by a quadruple of three variable functions as a diffeomorphism/mapping of $\mathcal{S}^3$ into Euclidian E^3 related to $\left(E_x = \rho\cos(\varphi)\sin(\theta), E_y = \rho\sin(\varphi)\sin(\theta), E_z = \rho\cos(\theta)\right)$ — spherical coordinates, where $0 \le \rho < \infty$, $0 \le \varphi \le 2 \cdot \pi$, and $0 \le \theta \le \pi$:

$$\left(\frac{2 \cdot \rho}{1+\rho^2} \times \cos(\varphi) \cdot \sin(\theta); \frac{2 \cdot \rho}{1+\rho^2} \times \sin(\varphi) \cdot \sin(\theta); \frac{2 \cdot \rho}{1+\rho^2} \times \cos(\theta); \frac{-1+\rho^2}{\rho^2+1}\right).$$

The partial derivatives of the projection/diffeomorphism represent the Jacobin matrix J, whereby its transpose J^T is given as follows:

$$\left\| \begin{matrix} 2\frac{1-\rho^2}{(1+\rho^2)^2}\times \\ \times\cos(\varphi)\sin(\theta) \end{matrix} & \begin{matrix} 2\frac{1-\rho^2}{(1+\rho^2)^2}\times \\ \times\sin(\varphi)\sin(\theta \end{matrix} & \begin{matrix} 2\frac{1-\rho^2}{(1+\rho^2)^2}\times \\ \times\cos(\theta \end{matrix} & \frac{4\cdot\rho}{(1+\rho^2)^2} \\ \begin{matrix} -\frac{2\cdot\rho}{1+\rho^2}\times \\ \times\sin(\varphi)\sin(\theta) \end{matrix} & \begin{matrix} \frac{2\cdot\rho}{1+\rho^2}\times \\ \times\cos(\varphi)\sin(\theta) \end{matrix} & 0 & 0 \\ \begin{matrix} \frac{2\cdot\rho}{1+\rho^2}\times \\ \times\cos(\varphi)\cos(\theta) \end{matrix} & \begin{matrix} \frac{2\cdot\rho}{1+\rho^2}\times \\ \times\sin(\varphi)\cos(\theta) \end{matrix} & \begin{matrix} -\frac{2\cdot\rho}{1+\rho^2}\cdot\times \\ \times\sin(\theta) \end{matrix} & 0 \end{matrix} \right\|$$

Consequently, Gram Matrix as the space metric tensor $G_{i,j} = J^T \times J$ yields

$$G_{i,j} = \frac{4}{(1+\rho^2)^2} \times \left\| \begin{matrix} 1 & 0 & 0 \\ 0 & \rho^2\sin^2(\theta) & 0 \\ 0 & 0 & \rho^2 \end{matrix} \right\|,$$

which leads to the metric rod $dl^2 = \frac{4}{(1+\rho^2)^2}\left[d\rho^2 + \rho^2\left(\sin^2(\theta)d\varphi^2 + d\theta^2\right)\right]$.

4.4. Foundation of Planck satellite data in terms of stereographic projection

Before approaching this issue, it is necessary to start calculating the volume of 3-dimensional regions in our 3-dimensional Euclidean plane. It is easy to verify that the volume of the entire space is equal to $\lim \boldsymbol{S}^3(\rho)$ as $\rho \to \infty$, namely $\boldsymbol{S}^3(\infty) = 2\cdot\pi^2$. Now it remains for us to calculate which part in percentage is the volume $V.\boldsymbol{S}^3(\rho)$ in relation to $2\cdot\pi^2$. The following mathematical sequence is reduced to the following chain of formulas.

We know that in flat E^3 topology, the rod volume dl^3 is equal to $dx \cdot dy \cdot dz$, whereas the rod length is given by $dl^2 = dx^2 + dy^2 + dz^2$. Applying the same rule to the previous flat expression for dl^2, we obtain

$$dl^3 = 8 \cdot \frac{\rho^2 d\rho \cdot \sin(\theta) d\theta \cdot d\varphi}{\left(1+\rho^2\right)^3},$$

within a coordinate triple: $0 \le \rho < \infty$, $0 \le \theta \le \pi$ and $0 \le \varphi \le 2\pi$. Hereby the expression

$$8\int_0^{2\pi} \int_0^{\pi} \int_0^{\rho} \frac{\xi^2 d\xi \cdot \sin(\theta) d\theta \cdot d\varphi}{\left(1+\xi^2\right)^3}$$

in the form of integral represents the space volume $V.\mathcal{S}^3(\rho)$ of a hyper-manifold $\mathcal{S}^3(\rho)$ with a radius ρ.

The *radius* $r = \dfrac{2 \cdot \rho}{1+\rho^2}$ can be interpreted as a new dimension, implying that the space volume is proportional to Euclidian space E^3 at nearby distances. Taking the integral into account, we derive the expression of the volume:

$$V.\mathcal{S}^3(\rho) = 4\pi \cdot \frac{-\rho + \tan^{-1}(\rho) + \tan^{-1}(\rho) \cdot \rho^4 + \rho^3 + 2 \cdot \tan^{-1}(\rho) \cdot \rho^2}{\left(1+\rho^2\right)^2}.$$

After accounting for the sub-expression $\tan^{-1}(\rho)$, we obtain

$$V.\mathcal{S}^3(\rho) = 4\pi \cdot \frac{\left(1+\rho^4+2 \cdot \rho^2\right)}{\left(1+\rho^2\right)^2} \cdot \tan^{-1}(\rho) + 4\pi \cdot \frac{-\rho+\rho^3}{\left(1+\rho^2\right)^2}.$$

Finally, we arrive at $$V.\mathcal{S}^3(\rho) = 4\pi \cdot \left(\tan^{-1}(\rho) + \rho \cdot \frac{-1+\rho^2}{\left(1+\rho^2\right)^2} \right).$$

To interpret the stereographic projection in order to confirm to the matter Composition put forward by the Planck Mission 2013 satellite data it is necessary to establish the share of the volume $V.\mathcal{S}^3(\rho)$ with respect to the entire volume $\mathcal{S}^3(\infty) = 2 \cdot \pi^2$. Indeed, while the share

$$sh(\rho) = \frac{2}{\pi}\left(\tan^{-1}(\rho) + \rho \frac{-1+\rho^2}{\left(1+\rho^2\right)^2} \right), \; sh(\infty) = 1.$$

At https://sci.esa.int/web/planck/-/51557-planck-new-cosmic-recipe, we read *"Planck's high-precision cosmic microwave background map has allowed scientists to extract the most refined values yet of the Universe's ingredients. Normal matter that makes up stars and galaxies contributes just 4.9% of the Universe's mass/energy inventory. Dark matter (quantum vacuum, ed.), which is detected indirectly by its gravitational influence on nearby matter, occupies 26.8%, while dark energy, a mysterious force thought to be responsible for accelerating the expansion of the Universe, accounts for 68.3%."* accessed online 26/07/2022.

This understanding brings about not only one but also two divisions of the same metric as two different solutions of the equation $\mathrm{sh}(\rho_0) = 0.268$ for $\rho_0 = 0.675545953$, and $\mathrm{sh}(\rho_1) = 0.951$ for $\rho_1 = 3.069027963$. One can check that for dark matter or **Qv**-vacuum, and for baryonic or normal **Vm**-matter bubbles respectively, $0 \le \varphi \le 2\pi$, $0 \le \theta \le \pi$.

Qv:	**De:**	**Vm**:
$\mathrm{sh}(\rho_0) = 0.268$	$\mathrm{sh}(\rho_1) - \mathrm{sh}(\rho_0) =$ $= 0.683$	$\mathrm{sh}(\infty) - \mathrm{sh}(\rho_1) =$ $= 0.049$
$0 \le \rho < \rho_0 =$ $= 0.675545953$	$\rho_0 \le \rho < \rho_1 =$ $= 3.069027963$	$\rho_1 \le \rho < \infty$

Table 1: Stereographical Composition: **Qv-** as quantum vacuum, **De-** as dark energy.

Finally, it remains for us once again to pay attention to the connection between the metric space, which is a stereographic projection, and the original (pre-image) defined by the Landau-Lifshitz metric (1). As already noticed, in metric (1), there seem to be two bubbles extending along the coordinate r when moving along r from zero to 1, and in the opposite direction from 1 to zero. This movement along the coordinate r will be clear from the substitution $r = \dfrac{2 \cdot \rho}{1 + \rho^2}$ when moving along the coordinate ρ within the stereographic interval $[0 \le \rho < \infty)$. In stereo-

graphic projection, as said, these two bubbles are clearly separated by the transition boundary when $r = 1$. In metric (1), however, these two bubbles are superimposed on each other and each of which has a volume of π^2.

In order to be convinced of the above, we need to calculate the volume of the three-dimensional manifold $V.\mathcal{S}^3(r)$, which extends in metric (1) in the interval $[0, r)$. Indeed

$$V.\mathcal{S}^3(r) = \int_0^{2\pi} \int_0^{\pi} \int_0^{r} \frac{\xi^2 d\xi \cdot \sin(\theta) d\theta d\varphi}{\sqrt{1-\xi^2}} = 2 \cdot \pi \cdot \left\{ \sin^{-1}(r) - r \cdot \sqrt{1-r^2} \right\}$$

We can check that for quantum vacuum $\rho_0 = 0.675545953$ and for normal matter $\rho_1 = 3.069027963$

$$\frac{V.\mathcal{S}^3\left(r_0 = \frac{2 \cdot \rho_0}{1+\rho_0^2}\right)}{2 \cdot \pi^2} = 0.268 \text{, and } \frac{V.\mathcal{S}^3\left(r_1 = \frac{2 \cdot \rho_1}{1+\rho_1^2}\right)}{2 \cdot \pi^2} = 0.049 .$$

5. THE Γ-EQUATION

In connection with what will be said, it is necessary to make the following remark, which would be clear to the bartender. We often use this method of our narration wherever it is convenient.

Bartender physics. *It is not a secret that when watching a figure skater who, with a sharp effort or push, having stretched her arms as far as possible from the body, she sets a rotational movement to the whole body. Then controlling her movement, she begins to reduce the arms span, gradually pressing her hands closer and closer to her body, thereby involving her body in an accelerating rotational movement.*

If we now turn to the atomic model of Niels Bohr, then the "aging of atoms" from this bartender point of view may well be associated with a redshift. Following the energy conservation law hereby happens a potential energy loss of atoms by

gradual or sequential transition of the initial BB push of this potential energy into kinetic energy. Indeed, it is clear that a quantum of light or a photon's outflow (quantum transition) in distant orbits of atoms will have a longer wave and thus should carry less energy propagating in the space in contrast to young atoms against old ones. The so-called Niels Bohr orbits of electrons revolving around the nucleus will be closer to the nucleus for older atoms. Thus, the outflow of energy, as we move from large values of z *to smaller values, will gradually or sequentially increase for photons enclosed in light rays born in galaxies at huge cosmological distances ("young atoms"), as we move towards the galaxies closest to us ("older atoms"). We will see later the average potential energy density* μ *parameter simulation in the entire Universe by function* $1-(½)^z$ *meaning the decrease of* μ.

In formulating speculations similar to, cf. a) Mullat (1995), using the Γ-equation describing the current mass-energy composition in the Universe, our aim is to identify some stable states embedded into the four-dimensional hyper-globe $\mathcal{R}^4$ of a curvature radius 1 given by $x^2+y^2+z^2+r^2=1$ as topologies among three-dimensional ordinary manifolds $\mathcal{S}^3(r)$ of radius r, $0 \le r \le 1$, $x^2+y^2+z^2 \le r^2$.

The Copernican Principle, as an ideal attribute, can be assigned with two-dimensional surface $\mathcal{S}^2$ of a three-dimensional globe $\mathcal{R}^3$. Extending the Principle to the manifold $\mathcal{S}^3$ enclosing a hyper-globe $\mathcal{R}^4$, we preserve the same ideal properties. Therefore, stereographic $\mathcal{S}^3(\rho_0)$, $\mathcal{S}^3(\rho_1)$ embedded into hyper-globe $\mathcal{R}^4$ corresponds to the Principle idealizing homogeneity and isotropy of the Universe. Before proceeding further with the analysis, we will present a hypothetical situation based on the assumption that the Copernican Principle is an ideal absolute.

We assume that closed three-dimensional stereographic $\mathcal{S}^3(\rho)$ manifolds of radius ρ, $0 \le \rho \le \infty$, are surrounded by energy-field within the globe $\mathcal{R}^4$ of curvature radius 1. It should be reiterated that the observer does not necessarily have to be placed at the North Pole of $\Re^4$. However, we shall adopt $(0,0,0)$ in $\mathcal{S}^3(\rho)$ as the stereographic reference system origin O, while allowing the observer to be positioned at any point within the manifold $\mathcal{S}^3(\rho)$. Such representation, however, ignores

explanations of some known observational anomalies, such as super-void areas in Cosmos, local zones with higher and lower density of matter, etc. as anomalies in gravitational transitions of energy-field into quantum vacuum and baryonic matter.

According to Newton's laws, if a mass M of radius r hypothetically converges into a zero point O, the potential energy of a gravitational field at a distance r from O equals $-G\frac{M}{r}$, where $G = 6.67384^{-11}$ $m^3kg^{-1}s^{-2}$ is the gravitational constant. We can further hypothesize the process of gravitational transition, which occurs within the manifold $S^3(r)$—that is, at a distance r from some origin O. It is plausible to speculate that, at a distance r from the origin O, the energy-field gravitational transition takes place if the potential gravitational field intensity is strong enough—e.g. below the value of the universal constant Λ, i.e., at $-G\frac{M}{r} \leq -\Lambda$. The energy-field space and baryonic matter creation, according to our speculative postulate, is thus determined by a Γ-equation $-G \cdot M + \Lambda \cdot r = 0$. As previously noted, once the process of space or matter creation begins, it cannot cease or be arrested because by supposition a fixed point equilibrium should be reached, i.e., an increase in the mass M used in solving the Γ-equation in fact is increasing in a higher order than the increase in radius r needed for the mass M to be stipulated by the Γ-equation solution.

In the context of the gravitational constant G and the speed of light constant c may be omitted. Indeed, these parameters can be instead incorporated into the energy density μ, referring henceforth to energy $\mathcal{E}$ as $\mathcal{E}_{rel}$. Here, with respect to the manifold, the numerical values of energy $\mathcal{E}_{rel}$ are of key importance. Whether we refer to it as energy or by any other nomenclature is irrelevant for our theoretical purposes, as the gravitational constant G and speed of light c, as said, can be the built-in by the scale of Joule per kg. of the energy density parameter μ.

Let us now turn attention to the potential energy level on the manifold that forms the three-dimensional vectors (x, y, z) denoting manifold $\mathcal{S}^3$. In fact, these vectors represent the level of potential energy at the distance r from the centum of the manifold $\mathcal{S}^3(r)$ of radius r. As already emphasized by our speculative postulate, the space-energy composition undergoes gravitational transition, which allegedly occurs on the three-dimensional manifold embedded into the four-dimensional hyper-globe denoted by $\mathcal{R}^4$.

At last we are ready to introduce a parameter λ, allegedly representing a fine-tuning or calibrating parameter of the energy-field defined by Newton's formula. It features in the *"potential energy"* $-\frac{G \cdot \mathcal{E}}{c^2 \cdot r^\lambda}$ or $-\frac{\mathcal{E}_{rel}}{r^\lambda}$ modified, what being said, as in MOND model, Milgrom (1983). In accordance with the Speculation on the space-energy composition, transition occurs at the energy level equal to $-\Lambda$ representing some universal constant, as discussed above. Thus, the gravitational transition occurs by violating the Γ-equation $-\frac{\mathcal{E}_{rel}(r)}{r^\lambda} + \Lambda = 0$, where $\mathcal{E}_{rel}(r)$ corresponds to the energy $\mathcal{E}_{rel}$ of the manifold $\mathcal{S}^3(r)$. This equation describes the stable set applied to the space-energy composition. In the subsequent analyses, we will replace $\mathcal{E}_{rel}$ by its energy $\mathcal{E}_{rel} = V.\mathcal{S}^3(r) \cdot \mu$ of a manifold $\mathcal{S}^3(r)$ or total energy of a hole or bubble within an allegedly layering/inflating energy-field, where $V.\mathcal{S}^3(r)$ signifies the total volume of $\mathcal{S}^3(r)$. Note that we previously referred to the parameter μ as average of potential energy density. Hence, the product of μ and volume $V.\mathcal{S}^3(r)$ corresponds to $\mathcal{E}_{rel}$ — energy of the manifold $\mathcal{S}^3(r)$ under inflation. The parameter μ is of purely theoretical relevance, as it can neither be observed nor measured. Consequently, the Γ-equation might be rewritten in the form $-V.\mathcal{S}^3(r) \cdot \mu + \Lambda \cdot r^\lambda = 0$. In Section 7, we provide mathematical derivation of the equation upon our hyper-spherical manifold.

In accordance with **Γ**-equation the surface rod dl^2 of three-dimensional manifold $\boldsymbol{S}^3(r)$, $0 \le r < 1$, $0 \le \varphi \le 2\pi$, $0 \le \theta \le \pi$ yields a stereographical projection of $\boldsymbol{S}^3(r)$ given by

$$dl^2 = \frac{4}{\left(1+\rho^2\right)^2}\left[d\rho^2 + \rho^2\left(\sin^2\theta \cdot d\varphi^2 + d\theta^2\right)\right], \text{ where } r = \frac{2\cdot\rho}{1+\rho^2} \text{ and}$$

$0 \le \rho < \infty$, which guarantees that the manifold is mapped into a flat E^3 topology at nearby distances like a stereographical projection of S^3 from North Pole into Euclidian static space E^3. Hereby, the rod of the stereographical volume is defined by $dl^3 = \frac{8\cdot\rho^2}{\left(1+\rho^2\right)^3} d\rho \cdot \sin(\theta) d\theta \cdot d\varphi$, $0 \le \rho < \infty$, $0 \le \varphi \le 2\pi$ and $0 \le \theta \le \pi$. Consequently, the expression

$$8\int_0^{2\pi}\int_0^{\pi}\int_0^{\rho} \frac{\xi^2 d\xi \cdot \sin(\theta) d\theta \cdot d\varphi}{\left(1+\xi^2\right)^3}$$

represents the volume of radius ρ of hyper-manifold $\boldsymbol{S}^3(\rho)$ of ρ-*"radius"*. Taking the integral into account, we obtain:

$$V.\boldsymbol{S}^3(\rho) = 4\pi \cdot \left(\tan^{-1}(\rho) + \rho \cdot \frac{-1+\rho^2}{\left(1+\rho^2\right)^2}\right).$$

It thus can be easily verified that $V.S^3(\infty) = 2\pi^2$ represents the entire hyper-manifold volume. Hence, with regard to the **Γ**-equation, the equation can now be rewritten as:

$$\Gamma(\mu,\rho) = -4\pi \cdot \left(\tan^{-1}(\rho) + \rho \cdot \frac{-1+\rho^2}{\left(1+\rho^2\right)^2}\right) \cdot \mu + \Lambda \cdot \rho^{\lambda} = 0.$$

In order to calibrate **Γ**-equation, which must be taken as speculative, the roots must be accurately aligned with the latest Plank Mission data of the mass-energy composition in the Universe. In fact, **Γ**-equation can almost always be solved for two roots, where $\rho_0 < \rho_1$. The case with one root $\rho_0 = \rho_1$, as well as that described by $\rho_S = 0$, exists as well, as do those including no roots at all.

5.1. *Layering Dynamics of the Universe*

Imagine a globe $\mathcal{R}^3$; say of radius $r = 1$. Select any point on the surface of the ball and draw a circular area $\mathcal{S}^2$ around it. The layer $\mathcal{S}^2$ of a very small radius $0 < o << 1$ will now surround the point N. Increase o and draw a larger layer, i.e., encircle the layer around point N with increased radius o. Repeat this process until you reach the opposite side — the south pole of the ball. The entire ball $\mathcal{R}^3$ is now surrounded.

Conceive a globe; say in radius 1 and some black paint. Suppose that the black paint is a space under creation undergoing a gravitational transition from some latent energy-field. Choose any point at the globe surface and draw a circle of radius o around the point, e.g. encircle the point as the North Pole N. Then paint the circle inside this perimeter with black paint. Increase the radius o and draw a larger circle around the N point and once again cover the newly created area with black paint. Repeat this process until you reach the opposite side—the south S pole of the globe $\mathcal{R}^3$. The entire globe $\mathcal{R}^3$ is now black.

We established the *"layering dynamics"* of the universe as a hypothesis of gravitational transition exploiting a nomenclature of energy-field transition into quantum vacuum and baryonic matter without use of GR and time line as a sequence of 3-dimentianal surfaces/manifolds $\mathcal{S}^3$ of 4-dimentional globe $\mathcal{R}^4$. The dl^2 -s represent a stereographical projection of $\mathcal{S}^3$ with curvature 1 into Euclidian E^3 flat space; cf. Landau and Lifshitz, *"The Classical Theory of Fields"*, §107, p.348. The two roots ρ-s, ρ_0 and ρ_1 must resolve the Γ-equation:

$$\Gamma(\mu,\rho) = -4\pi \cdot \left(\tan^{-1}(\rho) + \rho \cdot \frac{-1+\rho^2}{\left(1+\rho^2\right)^2} \right) \cdot \mu + \Lambda \cdot \rho^{\lambda} = 0,$$

The roots $\rho_0(\mu)$ and $\rho_1(\mu)$ are exponential functions supporting the Universe growth with acceleration depending on average energy density μ while μ is linearly decreasing in semi-interval

$$\begin{pmatrix} \text{Planck Era} \rightarrow \mu \approx 10^{12} \geq \ldots \geq \mu \approx 10^{3} \leftarrow \text{Vacuum Ages Phase}, \mu \approx 0.12457 \\ \leftarrow \text{Current phase of Universe} \geq\geq \mu \approx 0.08727 \leftarrow \text{Final Death Phase} \end{pmatrix}.$$

Nothing can stop us from moving the $\mu \to \infty$ in such a way as to diminish the size of quantum vacuum or space bubble $S^3(\rho_0)$ by moving $\rho_0(\mu) \to 0$. This means that quantum vacuum bubble penetrates beyond the so-called Planck wall, with extent $\rho_0(\mu)$ smaller than the Planck constant $\hbar = 6.62606957 \cdot 10^{-34}$, can be included in our model.

By triple $\{\mu = 0.12457, \lambda = 0.83751, \Lambda = 0.91499\}$ we achieved the best match with Planck mission 2013 satellite data, i.e., matching 68.3% energy-field, 26.8% quantum vacuum and 4.9% baryonic matter using component function $\mathrm{sh}(\rho) = \frac{2}{\pi}\left(\tan^{-1}(\rho) + \rho\frac{-1+\rho^2}{\left(1+\rho^2\right)^2}\right)$. However, the capabilities of MathCad, which were used to calculate the table below, do not allow for technical reasons to calculate the solution of **Γ**-equation for $\mu > 10^{12}$.

Qv: *Quantum Vacuum*	**Be:** *Background Energy Field*	**Vm**: *Visual/Baryonic Matter*
$\mathrm{sh}(\rho_0) = 0.268$	$\mathrm{sh}(\rho_1) - \mathrm{sh}(\rho_0) = 0.683$	$\mathrm{sh}(\infty) - \mathrm{sh}(\rho_1) = 0.049$
$0 \le \rho < \rho_0 =$ $= 0.675545953$	$\rho_0 \le \rho < \rho_1 =$ $= 3.069027963$	$\rho_1 \le \rho < \infty$

$\mu \approx 10^{12}$, Planck wall Epoch or Era of the Big Bang	$\mu \approx 10^{3}$, The Universe quantum vacuum Phase	$\mu \approx 0.12457$, Current Phase of the Universe	$\mu \approx 0.087267626$, The Death Phase of the Universe
Quantum Vacuum/Space Composition			
$\mathrm{sh}(\rho_0)\% \approx$ $3.302832273 \cdot 10e - 17$	$\mathrm{sh}(\rho_0)\% \approx$ $\approx 0.000079175448461$	$\mathrm{sh}(\rho_0)\% \approx$ ≈ 26.784557217	$\mathrm{sh}(\rho_0)\% \approx$ ≈ 67.912846576
Background Energy-field Composition			
$\mathrm{sh}(\rho_1)\% - \mathrm{sh}(\rho_0)\% \approx$ $\approx 100\%$	$\mathrm{sh}(\rho_1) - \mathrm{sh}(\rho_0) \approx$ ≈ 99.9999208245515	$\mathrm{sh}(\rho_1) - \mathrm{sh}(\rho_0) \approx$ ≈ 68.300360425	$\mathrm{sh}(\rho_1) - \mathrm{sh}(\rho_0) \approx$ $\approx 0.00\%$
Visual or Baryonic Matter Composition			
$\mathrm{sh}(\infty) - \mathrm{sh}(\rho_1) \approx$ $\approx 0.00\%$	$\mathrm{sh}(\infty) - \mathrm{sh}(\rho_1) \approx$ $\approx 0.000000000000057$	$\mathrm{sh}(\infty) - \mathrm{sh}(\rho_1) \approx$ ≈ 4.914972357	$\mathrm{sh}(\infty) - \mathrm{sh}(\rho_1) \approx$ ≈ 32.087153424

Table 1: The function $\mathrm{sh}(\rho)$ readily explains the static space dynamics

The Table 1 understanding brings about not only one but also two divisions of the same metric as two different solutions of the equation $\mathrm{sh}(\rho_0) = 0.268$ for $\rho_0 = 0.675545953$, and $\mathrm{sh}(\rho_1) = 0.951$ for $\rho_1 = 3.069027963$. One can check that for the quantum vacuum or for the **Qv**-vacuum, and the baryonic or normal **Vm**-matter bubbles respectively, $0 \le \varphi \le 2\pi$, $0 \le \theta \le \pi$.

When the inflation time line in the Standard Model of the Big Bang began, column one defend our view that a positive root $\rho_0 \approx 0$ can be interpreted as infinitesimally small space volume of matter with radius $\rho_0 \approx 0$. As the SM inflation phase of the Big Bang developed further — the second column — the emergence of baryonic matter was lagged behind the appearance of quantum vacuum. We can rephrase this speculation believing that in the inflation phase only the quantum or vacuum space prevailed.

Column 3 (http://sci.esa.int/planck/51557-planck-new-cosmic-recipe/, last visited 24/12/2023) of the table shows an attempt to compare the composition of energy-field, quantum vacuum and baryonic matter, with satellite data. Despite the fact that satellite data were obtained on the basis of the SM, the most suitable parameters Λ, λ and μ with great accuracy fit into our phase transfer model as the basis for calculating distances to galaxies. Last column shows the death phase, when $\rho_0 \approx \rho_1$: the energy-field source will be almost exhausted—both the quantum vacuum and baryonic matter bobbles will start to slow down their alleged acceleration of growth.

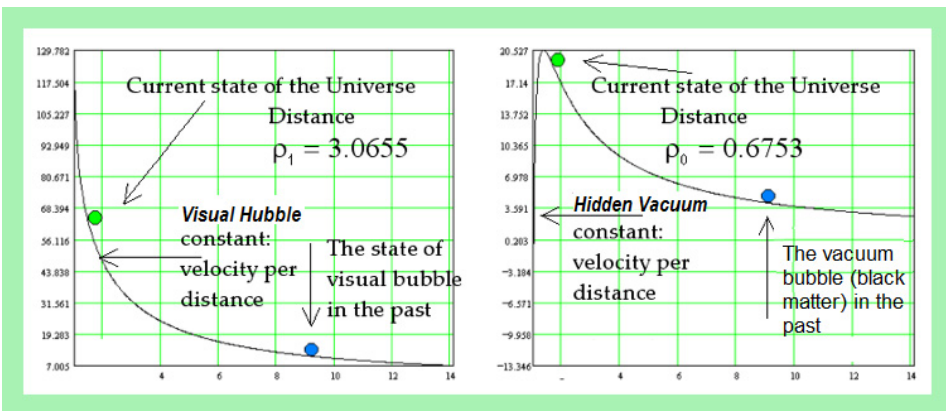

Fig. 2 and **Fig. 3:** Reveal the fundamental difference in the dynamics of quantum vacuum and baryonic matter highlighted in Table 1.

According to our analyses, which contradict the laws of gravity implying that the baryonic matter should start to contract, it allegedly continues to expand. This effect is readily apparent in the graphs depicted in Fig. 2 and Fig. 3. Indeed, they indicate that the baryonic matter creation velocity within the manifold $S^3(\rho_1)$ continues to accelerate, whereby as the manifold inflated with space continues to increase in size, the average energy density also decreases. However, when the energy density reaches the vicinity of the critical value κ, the alleged quantum vacuum $S^3(\rho_0)$ volume of quantum vacuum or space seem to be better aligned with the laws of gravity. Indeed, as shown in Figure 3, the creation of quantum vacuum does not stop although the acceleration completely stops before it becomes negative, that is, the growth of the radius of the quantum vacuum slows down, and the growth of its volume begins to slow down, respectively. So, in accordance with thermodynamic laws, in the vicinity of the critical value, as can be seen from Figure 3, the density of energy-field continues to decrease, but more slowly. We might thus conclude that the dynamics of the evolution of quantum vacuum and baryonic matter, accounting for the decreasing energy density, still corresponds to the known laws of physics.

5.2. Energy density scale construction

Parameters Λ, λ and μ represent a triplet in Γ-equation, where $-\Lambda$ is a mass-energy gravitational transition level, at which the transition occurs and which characterizes some speculative potential energy-field demarcation stripe on the scale inverse to radius ρ of the manifold S^3. Similarly, λ is a tuning or calibrating parameter for the postulated potential energy of the gravitation field itself, and μ denotes our speculative density of the manifold. By introducing the curvature of the manifold S^3 equal to 1, we have succeeded in calibrating the roots of the equation, which results in the following values for the aforementioned triplet: $\Lambda = 0.91499$, $\lambda = 0.83751$ and $\mu = 0.12457$. This parameter value set provides what being said the best fit to the Planck Mission Statement. It should be noted that we use a modified classical potential energy of gravitation field in the form of function $-\frac{\mathcal{E}_{\text{rel}}}{\rho^{\lambda}}$ that for $\lambda < 1$ declines more rapidly at nearby distances (i.e., when $0 < \rho \leq 1$) than for faraway distances (when $1 < \rho < \infty$).

Before we proceed further, it is necessary to establish the share of the volume $V.\mathcal{S}^3(\rho)$ with respect to the entire volume $V.\mathcal{S}^3(\infty) = 2\pi^2$ in order to conform to the quantum vacuum and baryonic matter composition put forth by the Planck Mission satellite data. Indeed, the share equals $\mathrm{sh}(\rho) = \frac{2}{\pi}\left(\tan^{-1}(\rho) + \rho \cdot \frac{-1+\rho^2}{\left(1+\rho^2\right)^2}\right)$. For the triplet given above, the roots $\rho_0 = 0.67535$ and $\rho_1 = 3.06548$ solve Γ-equation. It can, cf. Table 1, thus be verified that:

Quantum Vacuum / Space:	$Qv\% \mid \mathrm{sh}(\rho_0) \approx 26.785\%$,
Background / Energy-Field:	$Be\% \mid \mathrm{sh}(\rho_1) - \mathrm{sh}(\rho_0) \approx 68.300\%$,
Visual / Baryonic Matter:	$Vm\% \mid \mathrm{sh}(\infty) - \mathrm{sh}(\rho_1) \approx 4.915\%$.

These percentages in Table 1, with regard to the Plank Mission Statement, allow us to refer to ∞ as the baryonic matter crossing/starting point, which terminates at ρ_1. We can also refer to ρ_0 as the energy-field starting point, whereby the energy-field terminates when it reaches ρ_1, while the quantum vacuum commences at 0 and ends at ρ_0. The inverse stereographical distance $r_0 - r_1$ in r-reference system $r = \frac{2 \cdot \rho}{(1+\rho^2)}$ denotes the energy-field width. From the above, it can be inferred that, while the percentages align with the Planck Mission Statement nearly perfectly, the roots ρ_0 and ρ_1 produce a good fit only when $\mu = 0.12457$. Whatever this value μ of the energy density parameter represents or is interpreted to imply, the $\mu = 0.12457$ points at an alleged current density state of the Universe.

It remains for us to pay attention to the connection between the metric space, which is a stereographic projection, and the original (pre-image) defined by the Landau-Lifshitz metric:

$$dl^2 = \frac{dr^2}{1-\left(\frac{r}{a}\right)^2} + r^2 \cdot \left\{\sin^2(\theta) \cdot d\varphi^2 + d\theta^2\right\}.$$

The metric depends on the curvature radius a, where the r can vary from 0 to a, and where φ and θ are in the intervals $[0 \le \varphi \le 2\pi]$ and $[0 \le \theta \le \pi]$. In particular, we will work without any high rank tensors, time coordinate, laws of gravity, etc., focusing only on standard quadratic forms of differential geometry. This dl^2 was considered in "Classical Field Theory", Landau-Lifshitz (LL), 3rd Revised English Edition, 1971, p. 336. According to LL, the substitution $r = r_1 \cdot \left(1 + \frac{r_1^2}{4 \cdot a^2}\right)^{-1}$ for $0 \le r_1 \le a$, would at every point of a 3-d manifold $\mathcal{S}^3$ lead to

$$dl^2 = \left(1 + \frac{r_1^2}{4 \cdot a^2}\right)^{-2} \cdot \left(dr_1^2 + r_1^2 \cdot d\theta^2 + r_1^2 \cdot \sin^2\theta \cdot d\varphi^2\right).$$

By substitution $r_1 = 2 \cdot a \cdot \rho$ the LL metric can be converted exactly into our stereographic metric for $a = 1$, p.141. Now, moving $r = \frac{2 \cdot \rho}{1 + \rho^2}$ from $r = 0$ to 1 (hence moving $\rho = 0$ to 1), and then backwards moving $r = 1$ to 0 (hence moving $\rho = 1$ to ∞) it appears to be two bubbles inside the stereographic interval $[0 \le \rho = 1 < \infty)$. At this interval, these two bubbles are spaced along the boundary $\rho = 1$ in such a way that the bubbles overlap each other at every point at a distance r from the common Center$(0,0,0)$. The volume of each bubble is equal to π^2.

In order to be convinced of the above, we need to calculate the volume of the manifold $V.\mathcal{S}^3(r)$ within LL metric in interval $[0, r)$. Indeed

$$V.\mathcal{S}^3(r) = \int_0^{2\pi} \int_0^{\pi} \int_0^{r} \frac{\xi^2 d\xi \cdot \sin(\theta) d\theta d\varphi}{\sqrt{1 - \xi^2}} = 2 \cdot \pi \cdot \left\{\sin^{-1}(r) - r \cdot \sqrt{1 - r^2}\right\}.$$

We can check that for vacuum $\rho_0 = 0.675545953$ and for normal matter $\rho_1 = 3.069027963$

$$\frac{V.\mathcal{S}^3\left(r_0 = \frac{2 \cdot \rho_0}{1 + \rho_0^2}\right)}{2 \cdot \pi^2} = 0.268 \text{ and } \frac{V.\mathcal{S}^3\left(r_1 = \frac{2 \cdot \rho_1}{1 + \rho_1^2}\right)}{2 \cdot \pi^2} = 0.049.$$

5.3. Energy density scale of origin

The conclusion made here is based on the premise that, in line with our Speculation, the manifold composition must stop changing when the energy density declines below the threshold $\mu = 0.08727$. In this case, the quantum vacuum will *collapse into or be in contact* with the visible manifold when $\mu \approx 0.08727$ because $\rho_0 \approx \rho_1$. By implementing a ratio scale of density on the μ-axis as a ratio of density μ to somewhat critical density κ, i.e., $\frac{\mu}{\kappa}$, while moving from higher to lower density values, the roots should confirm, or at least not contradict, the currently accepted statements about the Universe dynamics.

Let us now introduce a scale that commences at the point corresponding to the critical density ratio $\frac{\mu}{\kappa} \approx 1$, $\kappa \approx 0.08727$. The manifold points on this scale at the ratio $\frac{\mu}{\kappa} \approx 1.42751$ as the current composition. In contrast, when very high values $\frac{\mu}{\kappa}$ are exceeded on the density scale, a small or infinitely small clump of quantum vacuum can suddenly undergo an initial gravitational transition from the zero solution $\rho_S = 0$ of our speculative Γ-equation, yielding $\mathrm{Hv}\% \approx 3{,}30283 \cdot 10^{-17}\%$ of the quantum vacuum and $\mathrm{Vm}\% \approx 0.00 \cdot 10^{-17}\%$ for the visual or baryonic matter. This fits well with the current postulate on the beginning of *"Dark Ages of the Universe"*, Trimble (1987), indicating that background energy-field $\mathrm{Be}\% \approx 100\% - 0.00 \cdot 10^{-17}\%$ constitutes almost the entire manifold, as illustrated by Figure 7 in the Appendix. At the other end of the scale the alleged composition suggests $\mathrm{Vm}\% \approx 32.67\%$ and $\mathrm{Hv}\% \approx 67.33\%$, when density decreases, and thus starts approaching the critical level $\kappa \approx 0.08727$, the roots of the equation cease to exist.

The roots of our speculative Γ-equation do not contradict, but rather confirm the *"flatness problem"* $\Omega_0 \approx 1.0002 \pm 0.0026$ of the Universe on traditional density scale Ω, when it is outside the generally accepted

critical density $\Omega \approx 1$, to expand forever, as was assumed in the Standard Model. Indeed, the similarly $\frac{\mu}{\kappa} \to 1$ with the last possibility for finding the roots of Γ-equation is reached when the width $\rho_0 - \rho_1$ of the energy-field will approach zero.

5.4. Redshifts transformation into energy density scale.

Invariance is one of the fundamental properties of the energy density scale (as well as any other scale), since it allows linear transformations to be implemented, supporting the theoretical construction irrespective of the chosen scale interval. Here, we will illustrate the invariance by a linear transformation of distances into the scale of average densities of space and matter substituting the resulting densities μ in the equation

$$\Gamma(\mu,\rho) = -4\pi \cdot \left(\tan^{-1}(\rho) + \rho \cdot \frac{-1+\rho^2}{\left(1+\rho^2\right)^2} \right) \cdot \mu + \Lambda \cdot \rho^{\lambda} = 0,$$

where $\Lambda = 0.91499$ and $\lambda = 0.83751$. In solving this equation with respect to distances ρ, we obtain a theoretical distribution of distances, which will be appropriately compared with the distances in the original *Mean (MpC)* column of NED data with 15000 records; cf. Table 4 below.

First we return to the question of the average density of energy in the Universe. As already noted, when estimating the energy density, it was relatively easy to take into account the *"independent distances"* given in +/- percentages of Table 3 of +over/–under estimates below. It was also comparatively straightforward to transform the distances into the light years time scale indicating the propagation of light through static space until light from extragalactic objects reaches the telescope of the observer. In making this connection, it was also plausible to accept that light from extragalactic objects, indicated by column *Mean (MpC*), was emitted at some point in the past, with such various moments of origin denoted as $[\tau_o, \tau_n]$ representing some interval determined by the closest and the farthest object in the column *Mean (MpC)*. On the other hand, we have repeatedly pointed out the theoretical possibility of describing

events in static space by the energy density μ dynamics of energy distribution in the Universe. Thus, at this juncture, it should be clear that our reasoning leads to the emergence of a certain interval $[\mu_o, \mu_n]$ of average densities μ. Indeed, given that $\Lambda = 0.91499$ and $\lambda = 0.83751$, such an interval can be constructed, thus supporting our claim that average density can be used in place of the time scale events. These conditions result in obtaining solutions of **Γ**-equation that are reasonably matching with the +over/–under estimates in the *Mean (MpC)* column of Table 4.

To summarize the essence of calculating distances using **Γ**-equation, in accordance with the theory, it is necessary, what being said, to find a certain interval of energy densities $[\mu_o, ..., \mu_n]$, which would allow us to calculate distances. We do not have any methodology for choosing such an interval. All that can be counted on is a trial and error method. Nevertheless, as the trial and error method shows, it turned out to be necessary to consider three intervals on redshifts scale separated by two milestone points: $z_1 = 0.0015$ and $z_2 = 0.011118$. As a result, we have the opportunity to combine calculations into one procedure for calculating distances, both for small, moderate and significant redshift values. A similar separation of z values is already known for long time since the Hubble law is very accurately fulfilled for the small z values of redshifts. However, for large values, the Hubble's law validity is in doubt. The reader will be able to verify this further by viewing the Table 2.

Using the trial and error method for interval calibration, as we said, it was possible to separate the interval of redshifts into three extents. Based on our knowledge that for the Vacuum (Dark) Ages the energy density was $>> 0$ and for the Current Phase of the Universe the density is $\mu = 0.12457$ we succeeded in a rather satisfactory way. Indeed, given the redshift z in the interval $[z_o = 0 < ... < z_n = 10.99]$ we tried to estimate the density decrease in the form of $h(z) = 1 - \left(\frac{1}{2}\right)^z$ exponent's decay function in the following three cosmological redshifts extents:

$$[z_0 = 0 \le z < z_1 = 0.0015 \le z < z_2 = 0.11118 \le z < z_n = 10.99].$$

In each extent we implemented a separate linear transformation of z's using linear functions:

$$\mu(z) = \begin{cases} 98.188007 \cdot h(z) + 0.16027 \text{ for } z \in Z_1 = [z_0 = 0 \le z < z_1], \\ 97.926578 \cdot h(z) + 0.42157 \text{ for } z \in Z_2 = [z_1 \le z < z_2], \\ 102.812981 \cdot h(z) + 0.53757 \text{ for } z \in Z_3 = [z_2 \le z < z_n = 10.99]. \end{cases}$$

As the experiments show, it was prudent to apply a smoothed function: $\bar{\mu}(z) = \frac{1}{3} \cdot (\mu(z - 0.0001) + \mu(z) + \mu(z + 0.0001))$.

Distance Calculation Procedure. It remains thus to solve the equation $\Gamma(\bar{\mu}(z), \rho) = 0$ for $\bar{\rho}(z)$ depending on $z \in Z_1, Z_2$ or $z \in Z_3$. Then, the estimated distance to an extraterrestrial object equals $\bar{\rho}(z) - \rho_1$, where $\rho_1 = 3.065505$. We can now put on trial the distance $\bar{\rho}(z) - \rho_1$ given in MpC against Hubble and modulus $m - M$ distances, and also put on trial $\bar{\rho}(z) - \rho_1$ with reg. to formula of Noble Forrest W. & Timothy M. Cooper, 2014, http://www.pantheory.org/HF.htm, accessed 21.08.2018).

6. Results

Our contemporary knowledge of the structure of the Universe extends to galaxies and quasars, which form groups and clusters of various categories of extragalactic objects. The entire Cosmos is permeated with radiation comprising of the infrared, visible, ultraviolet and X-ray radiation emitted by extragalactic objects, as well as neutrino fluxes. It also includes relict microwave and neutrino radiation, the occurrence of which is purported to be associated with the *Big-Bang* event that initiated the emergence or grows of the Universe.

The complexity of the Universe, which we are trying to understand, and whose visual particles we strive to control, inevitably results in difficulties in attempting to represent observations in the field of astronomy in a form that is understandable to a mathematician. We hope that our mathematical modeling succeeded in overcoming such challenges, as it permits similar language to be adopted by both the observer and

the theoretical physicist. In creating this connection, we relied on the energy density μ parameter, developed in the previous section, which replaces the events in static space by energy dynamics of the Universe. It nonetheless explicates the distribution of matter and energy in the Universe that is acceptable to both mathematicians and physicists.

The energy density scale μ remains merely of theoretical value in spite of confirmation of the scale obtained by solving Γ-equation, for which we utilized the data sourced from NED distances in the form given by Table 2; cf. Astronomical Journal, 153:37 20 pp. (Steer et al. 2017). On the other hand, the scale μ explaining the dynamics of the Universe in alternative terms related to extragalactic objects can be interpreted as evidence supporting the reliability of our mathematical model, rather than pointing to its inconsistency.

6.1. NED Data

For the comparative analysis, in line with the approaches described in known literary sources, cosmic distances are traditionally calculated using: relativistic Doppler Effect formula with the Hubble constant H_0 or the formula for modulus $m - M$. However, Noble et al. distance, http://www.pantheory.org/HF.htm (accessed 21.08.2018) is different. It is noteworthy that in Table 2 by specifying the redshift z the distance to a cosmological object allows to be expressed in megaparsecs, also known as the MpC distance. It signifies the position to which the object should be repositioned in order to see it at an angle of 1″ second from the protozoan points of the Earth's orbit around the Sun.

Table 2: Intergalactic estimates: Representatives of Galaxies	**Equa-tion**	**Hubble**	**F. Noble**	**M-Distance**	**Mean m - M**	**NED (MpC)**	**Window**
MACS J0647.7+7015	**9643.0**	**4046.1**	**25338.4**	**46410.6**	**47.8104**	**7415.3**	Win1
GRB 060210	**8897.1**	**3851.2**	**16999.0**	**29795.2**	**47.1553**	**6680.1**	Win2
GRB 060526	**8418.4**	**3768.6**	**14351.3**	**19561.4**	**45.9457**	**4946.3**	Win3
GRB 030429	**7799.9**	**3595.7**	**11917.0**	**20218.6**	**46.3504**	**5649.6**	Win4
[HB89] 2345+000:BX0120	**7326.2**	**3440.8**	**10468.6**	**16720.6**	**45.7164**	**4350.7**	Win5
GRB 030226	**6489.0**	**3228.8**	**8426.9**	**12372.6**	**45.1692**	**4465.3**	Win6
COMBO-17 19434	**5895.5**	**3093.4**	**7244.9**	**9358.4**	**44.6939**	**3568.7**	Win7
COMBO-17 40328	**5455.3**	**3053.1**	**6468.1**	**9351.9**	**44.7727**	**4036.4**	Win8

COMBO-17 35663	**5232.3**	**2949.9**	**6100.8**	**9031.7**	**44.6779**	**3957.9**	Win9
SCP 06R12	**4798.6**	**2769.1**	**5430.5**	**7450.9**	**44.2321**	**3476.1**	Win10
GRB 000911	**4469.3**	**2683.1**	**4954.9**	**6561.9**	**43.9983**	**3225.9**	Win11
GSS 074_5532	**4325.7**	**2629.8**	**4755.4**	**8202.0**	**44.2812**	**3836.4**	Win12
[RSC2007] J123809.00+621847	**4246.1**	**2601.4**	**4646.9**	**6592.2**	**44.0283**	**3295.2**	Win13
XSS J18076+5937	**4195.1**	**2601.8**	**4578.1**	**5980.3**	**43.8316**	**3053.7**	Win14
GRB 071010B	**4132.7**	**2551.1**	**4494.6**	**5828.2**	**43.7528**	**3013.9**	Win15
CGCG 266-031	**98.2**	**102.1**	**107.9**	**104.5**	**35.0596**	**102.0**	Win184
UGC 11064	**96.0**	**100.4**	**105.2**	**144.4**	**35.3321**	**103.7**	Win185
ESO 573- G 014	**93.5**	**97.6**	**102.3**	**114.8**	**35.0979**	**112.2**	Win186
NGC 0232	**90.0**	**92.9**	**98.0**	**104.9**	**34.9671**	**96.0**	Win187
UGC 06363	**86.2**	**88.9**	**93.4**	**169.5**	**35.0541**	**92.1**	Win188
ESO 300- G 009	**82.8**	**85.1**	**89.3**	**90.6**	**34.7375**	**88.7**	Win189
NGC 3332	**79.4**	**81.0**	**85.1**	**107.3**	**34.7433**	**82.6**	Win190
NGC 3873	**75.6**	**77.4**	**80.5**	**72.6**	**34.2727**	**71.3**	Win191
UGC 00052	**74.3**	**75.3**	**78.9**	**71.8**	**34.2273**	**70.6**	Win192
ESO 478- G 006	**71.4**	**71.0**	**75.2**	**73.8**	**34.3151**	**72.5**	Win193
NGC 5490	**68.5**	**68.2**	**71.7**	**78.0**	**34.2991**	**68.7**	Win194
CGCG 141-044	**67.0**	**66.0**	**69.8**	**70.5**	**34.1464**	**69.4**	Win195
NGC 4495	**65.7**	**65.0**	**68.1**	**64.2**	**34.0064**	**63.1**	Win196
UGCA 036	**63.7**	**62.4**	**65.7**	**64.4**	**33.9964**	**63.5**	Win197
CGCG 308-009	**61.9**	**60.1**	**63.3**	**64.5**	**34.0033**	**63.5**	Win198
NGC 2258	**58.4**	**56.0**	**58.9**	**59.0**	**33.8212**	**58.2**	Win199
NGC 7408	**46.8**	**47.6**	**50.4**	**49.0**	**33.4045**	**47.1**	Win200

The data in Table 2 is collected on the basis of individual cosmological objects from NED sources. As far as we know, the NED database is provided by long-term observations conducted by astronomers, institutions, individual research groups, or private organizations interested in space depth research. The distances and the modulus are of interest for evaluating and comparing the theoretical methods. However, this still does not alleviate the bewildering and perplexing problems related to calculating distances to cosmological objects. According to NED, for galaxies or stars the distances are measured independently of redshifts. However, it seems to us that m – M modulus have been frequently used for this purpose, probably due to the challenges related to conducting independent measurements at the distant parts of the Universe.

When moving along the 15.000 lines in the MS *EXCEL* spreadsheet, the mean and median values of averages for 200 windows were calculated. Each window consists of 75 supernova records. Comparative results of distances are presented in Table 2. The entire table is available on request. We have chosen these windows for some technical reasons connected to MathCAD 5.0, which allows vector variables at most only with 200 components to solve equations by iteration method.

For comparison, an index of distance +over/–under estimates for these 200 windows was developed. To produce a normalized index, we divided average distances D_i obtained by a particular method by the average NED distance N_i in Mean (MpC) column and then subtracted one. The indices $\left(\frac{D_i}{N_i} - 1\right)$, $i = \overline{1...200}$, of +over/–under estimates reflects the situation in Table 3 like a series of experiments have been conducted to determine whether the distances D_i are closer or further than the N_i distance shows. If the experiment shows a different results (more or less) equal number of times (closer or further), then it is considered that D_i is approximately balanced with an expected distance N_i. If it, also, almost always turns out that objects on trial are closer than (or farther than) N_i, then it is considered that the D_i distance, in contrast, is misbalanced with N_i.

It became clear for some astronomers, who postulate a link between intergalactic distance and the extent of redshift, observing the Universe on the basis of Hubble's law, that the calculations using the relativistic Doppler formula are not entirely correct. In order to examine this issue more closely, we calculated the mean and median +over/–under estimates of distances collected into Table 3 taken from 15.000 supernova records in NED database. Based on the information sourced from the database, using some H_0, we compared methods typically employed when calculating distances between the objects in the Universe. In Table 3, the Γ-equation column presents distances based on the μ scale, which we denoted as the energy density scale of space and matter.

Disbalance z>0.594	**29.4%**	**-21.7%**	**54.2%**	**121.1%**
Median z>0.594	**24.1%**	**-20.8%**	**31.2%**	**84.0%**
Deviation	0.14	0.07	0.51	0.98
Disbalance 0.594>=z>0.2178	**0.4%**	**-22.3%**	**1.7%**	**38.4%**
Median 0.594>=z>0.2178	**0.0%**	**-22.3%**	**1.7%**	**35.3%**
Deviation	0.09	0.07	0.10	0.18
Disbalance z<=0.2178	**0.8%**	**0.1%**	**5.3%**	**3.1%**
Median z<=0.2178	**0.1%**	**-1.3%**	**4.1%**	**1.7%**
Deviation	0.03	0.05	0.05	0.04
Table 3: Total Observation	**Γ**-equation	Hubble	Noble	Modulus

Closer scrutiny of the data presented in Table 3 reveals that, at lower, perhaps moderate, redshift values, i.e., for $0.594 \geq z > 0.2178$, there is reasonable agreement between the **Γ**-equation and Noble F. formula for the distances to cosmological objects. The quality of the computed distances is also compared by the alignment with the Doppler formula. However, for higher redshifts, i.e., for $z > 0.594$, discrepancies for **Γ**-equation with Doppler formula are evident, as well as in relation to the Modulus and the results based on the Noble et al. theory both together. Although Noble F., and Modulus seems to overestimate independent distances, the **Γ**-equation provides similar overestimates for greater redshifts. In addition, according to the Doppler Effect calculations based on the Hubble constants chosen from the range starting at 66.375 up to 70, the discrepancies of underestimates exist both at moderate and higher redshifts. Indeed, Hubble's law produces obvious underestimation for both of these indicated extents of redshifts. However, according to Table 3, for the redshift values $z \leq 0.2178$ pertaining to the cosmological objects *"in the vicinity"*, the **Γ**-equation predicted approx. the same magnitude of estimates relative to those yielded by luminosity distances. This prediction for galaxies in the nearest vicinity, as already noted, is often based that in the NED Database the estimates relay on modulus distance formula.

6.2. A Posteriors Experiment

The formulas of Hubble's law relativistic Doppler Effect in comparison to **Γ**-equation, are shown, F. Noble and Modulus distances, on Figure 4 — both in their original form and in a more elegant form.

Hubble Distance

$$\frac{(1+z)^2-1}{(1+z)^2+1}\cdot\frac{c}{H_0}$$

$$\tanh(\ln(1+z))\cdot\frac{c}{H_0}$$

Pan Distance $c = 299792.458$ **speed of light** $H_0 = 66.375$

$$21.2946\cdot\log\left[\frac{1}{2}\cdot\left[\left(\sqrt{1+z}\right)-1\right]+1\right]\cdot\left(\sqrt{1+z}\right)\cdot 1958.3$$

$$18110.607641\cdot\ln\left[\left(\frac{1+\sqrt{1+z}}{2}\right)^{\sqrt{1+z}}\right]$$

Modulus distance MpC

$$dist = \frac{10^{1+\frac{m-M}{5}}}{106}$$

Figure 4: The formulas for calculating distances to Cosmological Objects according to the methods known to the author of the study. The results yielded by applying these formulas are transferred into Table 4.

Table 4: For any astronomer, including amateurs, it will be easy to check our results if one tries to access the NED, https://ned.ipac.caltech.edu/forms/byname.html (accessed 12/19/2018), where one can find the redshift values for some extraterrestrial objects.

Γ-Eq.	Hubble	Noble	Modulus	Redshift	Extraterrestrial object
2171.9	1498.8	2197.6	2523.5	0.466082	3C 411
1701.3	1241.1	1715.1	1386.8	0.366090	3C 048
9237.2	3796.6	19714.9	24774.2	4.047950	GRB 060206
6697.3	3188.7	8887.9	13614.4	1.819000	3C 256
704.9	603.3	734.8	734.5	0.159492	3C 273
112.7	111.4	125.0	115.3	0.027514	NGC 4860
6057.2	3011.6	7550.3	11117.3	1.549480	GRB 051111
923.2	756.7	947.9	809.1	0.204885	LEDA 25177
103.7	102.2	114.4	102.8	0.025199	ARP 334
26.3	22.0	24.4	22.2	0.005380	ARP 152
24.9	20.1	22.2	16.4	0.004907	ARP 159
32.3	30.0	33.2	30.3	0.007331	NGC 0772
5218.3	2755.3	6078.4	8550.7	1.253328	GRB 020813
37.0	36.1	40.1	38.0	0.008836	NGC 3516
8.2	6.1	6.8	8.4	0.001491	NGC 5832
4151.6	2381.4	4519.9	5970.4	0.939227	AO 0235+164
3.1	3.3	3.6	6.7	0.000804	MESSIER 101
576.0	507.7	608.0	542.0	0.132313	LEDA 51975
78.5	75.4	84.1	77.3	0.018529	ARP 220
1.9	1.2	1.3	1.2	0.000297	NGC 4569
73.2	69.6	77.5	66.7	0.017085	3C 449
107.5	106.1	118.9	66.7	0.026175	NGC 7385
495.3	445.5	527.8	515.2	0.115068	PKS 2155-304
24.0	18.9	20.9	16.5	0.004622	NGC 4487
101.4	99.8	111.7	16.5	0.024601	NGC 1265
328.5	309.9	358.9	342.0	0.078548	IC 1101
6022.5	3001.6	7483.7	11015.4	1.536089	SDSS J1156+1911
138.0	136.9	154.1	137.4	0.033903	ESO 325- G 004
69.2	65.1	72.5	66.4	0.015980	ABELL 3627
71.1	67.2	74.9	67.0	0.016506	2MASS J04375556-0931094
52.5	46.2	51.3	46.8	0.011313	NGC 7714

95.2	**93.3**	**104.3**	**95.9**	**0.022980**	UGC 00014
9855.2	**3980.4**	**33262.1**	**68548.8**	**7.000383**	EGS-zs8-1
38.6	**38.1**	**42.3**	**28.2**	**0.009330**	NGC 7619
43.9	**44.9**	**49.8**	**45.5**	**0.010988**	NGC 5010
7414.9	**3371.7**	**10720.3**	**17139.6**	**2.189613**	UDFj 39546284
126.0	**124.9**	**140.4**	**130.0**	**0.030893**	Markarian 421
26.3	**22.0**	**24.4**	**22.2**	**0.005380**	NGC4486
31.1	**28.4**	**31.4**	**28.7**	**0.006940**	LEDA 36252
111.3	**109.9**	**123.3**	**113.8**	**0.027140**	PGC 6240
9444.0	**3848.2**	**22067.6**	**3848.2**	**4.546953**	Baby Boom
823.7	**688.0**	**850.9**	**863.0**	**0.184268**	ABELL 1689
1474.7	**1108.4**	**1488.8**	**1606.9**	**0.318843**	ABELL 1995
3198.2	**1991.8**	**3330.3**	**4130.5**	**0.698091**	MACS J0744.9+3927
1520.1	**1135.5**	**1533.9**	**1667.2**	**0.328288**	ZwCl 1358.1+6245
61.1	**56.1**	**62.3**	**57.0**	**0.013746**	Hydra Cluster
4293.8	**2434.8**	**4711.9**	**3597.5**	**0.978000**	SN 2001jm
2635.1	**1732.0**	**2693.2**	**3062.0**	**0.568000**	SN 2001iy
6054.1	**3010.7**	**7544.2**	**11117.3**	**1.548267**	HG 051111
23.0	**17.6**	**19.4**	**16.8**	**0.004283**	MESSIER 87
30.2	**27.2**	**30.2**	**27.5**	**0.006658**	ARP 274
110.56	**109.2**	**122.46**	**124.7**	**0.026959**	NGC 4039
9100.4	**3764.0**	**18499.1**	**33265.9**	**3.792285**	N4C 41+41.17
54.1	**48.1**	**53.4**	**45.5**	**0.011778**	ARP 333
9776.5	**3943.7**	**28892.1**	**5495.4**	**6,027000**	ABELL 383
22.6	**16.93**	**18.7**	**11.8**	**0.004130**	ESO 162G017
7255.1	**3332.2**	**10273.2**	**16218.1**	**2.099000**	4C +01.02
7470.4	**3385.2**	**10881.8**	**17458.2**	**2.222364**	PKS 0237-23
9402.6	**3837.5**	**21530.0**	**16069.4**	**4.432400**	PSS J0747+4434
7895.6	**3486.9**	**12246.7**	**10280.2**	**2.500000**	B3 0727+409
9765.1	**3943.2**	**28842.2**	**24660.4**	**6.016000**	SDSS J1306+0356
1369.3	**1044.5**	**1384.5**	**1224.6**	**0.297000**	H 1821+643
9882.6	**3994.8**	**35505.5**	**31915.4**	**7.507800**	z8 GND 5296
9907.3	**4010.8**	**38529.5**	**17298.2**	**8.200000**	GRB 090423
9942.1	**4050.9**	**50744.0**	**50118.7**	**11.09000**	GN-z11
25.0	**20.2**	**22.4**	**20.3**	**0.004937**	NGC3227
76.1	**72.5**	**81.1**	**74.5**	**0.017877**	NGC5548
2745.0	**1784.6**	**2814.3**	**2432.2**	**0.592800**	3C 345
9886.6	**3997.2**	**35915.4**	**31188.9**	**7.601068**	ABELL 1689-zD1
9926.1	**4027.2**	**42444.3**	**40738.0**	**9.110000**	MACS1149-JD1

6.3. Summary

Summing up all our efforts presented in this study, we can conclude that the distances calculated in accordance with the Hubble's law are the most severely underestimated in almost entire spectrum of red-shifts. On the other hand, the deviations created by the Noble F. are an order of magnitude higher overestimates the greater are the redshift values even if they match quite satisfactory the NED Database for lower

values. When measuring distances using the modulus for estimating luminosity distances, the largest deviations, even grater than Noble F., occur in the spectrum of high redshifts.

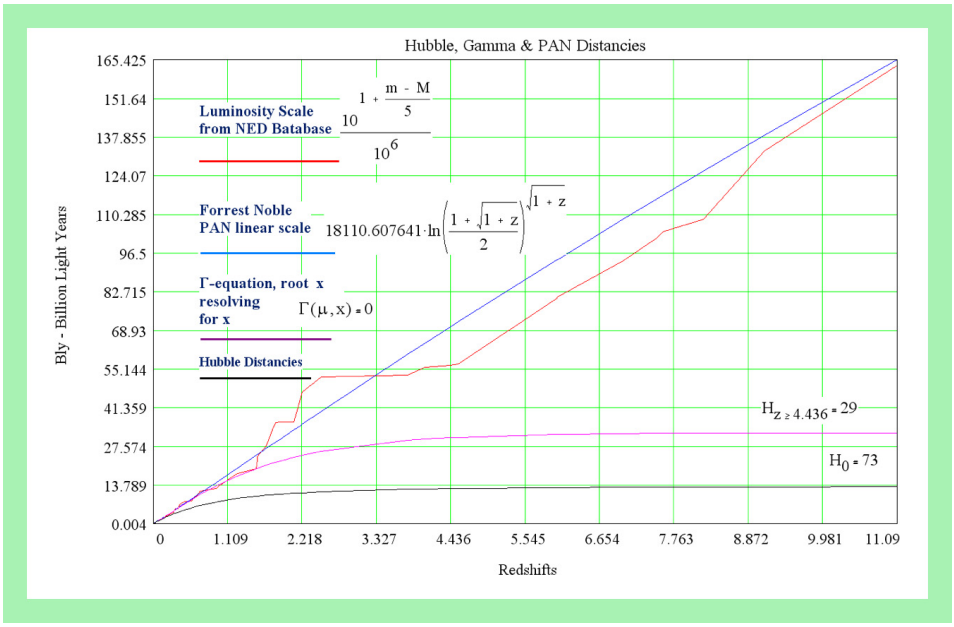

Figure 5: Based on cosmological redshifts z and modulus $m - M$ obtained from NED database. It is an image of the comparative analysis of distances calculated to cosmological objects on the basis of the formulas given above and **Γ**-equation procedure. The Luminosity, Noble F., Γ-eq., NED and Hubble traces are calculated using Table 2. Substituting into the Noble formula $z = 1$, the distances are approximately consistent with the linear law: $\text{Linear Pan Formula}(z = 1) \cdot z$.

It should be noted that the estimates obtained using the **Γ**-equation are more reasonable in the spectrum of moderate redshifts than the estimates obtained by all other methods. The observation of the position of the **Γ**-equation estimates on the Figure 5 amid Noble F., and NED Database distances, also with regard luminosity distance, indicates for us that the size of the universe does not correspond well enough to the Hubble's law. If we take into account the reasonableness of our mathematical model in this study the Universe seems for us to be also much larger in size than it is commonly believed. Such a discrepancy in the estimates may well be due to the fact that the luminosity of

distant cosmological objects is much stronger than expected, and these distant objects emit, perhaps, much more energy. It is also noteworthy to emphasize that using the NED database it was possible to fine tune calculations and establish the most accurate estimates of the distances to cosmological objects by the Γ-equation. The tuning was achieved by dividing the redshifts interval into three extents introducing three average energy density functions separately in each extent as noted above.

In conclusion, it is also necessary to make, as we think, one important comment. We have repeatedly pointed to the Hubble's constant that this is not a constant at all, but most likely, a Hubble's variable H_0. If our thoughtful reader turns attention to the trace calculated by the rules of the Γ-equation, then one can see that this trace in Figure 5 is very similar to the Hubble's distances somewhere starting with the redshift values in the region higher than $z \approx 4.436$. The Hubble's trace occupy a shifted area along the y-axis but down by some interval. Now it is not difficult to figure out what will be the shift interval along the y-axis, which can match the Γ-equation trace into Hubble's trace by changing the constant H_0 for calculating distances using the formula:

$$\frac{(1+z)^2-1}{(1+z)^2+1}\cdot\frac{c}{H_0} \equiv \tanh(\ln(1+z)\cdot\frac{c}{H_0}.$$

Indeed, the current value of $H_0 = 73$, and c is the speed of light—the value 73 is taken from NED database. If we now replace the constant H_0 by $H_{z\geq 4.436} = 29$ (remembering that this is not a constant at all), then it turns out that the Hubble distance trace will very accurately fit our trace calculated according to the rules of the Γ-equation. However, we must separate the entire space of galaxies—if we may say so—into two regions—the so-called foreground galaxies with the red shift number with the boundary number no more than 4.436, and the background galaxies with the redshift number greater than 4.436. The indicated shift by 29 is valid only for background galaxies with a redshift of more than 4.436 and from which the light has reached us from the distant past. Now, again, it is not difficult to understand that if we take the

number 29 for the Hubble's constant, then it will be a constant, which supposedly was in the distant past and which tells us, presumably, that in the distant past the growth of the Universe occurred more than two times slower than now.

From the foregoing, it is quite obvious to conclude that it is also fully consistent with Figure 2, that in the modern era, according to the forecast calculated according to the rules of the Γ-equation, in the future our universe will expand faster and faster. Everything that has been said here (we have already indicated this circumstance where it was appropriate) agrees with the fact that the size of our universe not only increases, but this growth also occurs with acceleration. However, as the dynamics of acceleration shows, in accordance with the Γ-equation—the Γ-trace in the past—the growth of the Universe, as well as the acceleration, both have been practically insignificant. Indeed, for large values of redshift in the displacement of distances along the y axis, the Γ-trace is almost parallel to the x axis of the redshift.

It is also appropriate to emphasize here that the Γ-equation is derived from the postulate of the gravitational transition of energy-field into quantum vacuum and baryonic matter. Therefore, the growth of the Universe by the rules of the Γ-equation is not an expansion in the sense of the standard cosmological model, i.e., Big Bang model, but a certain growth of the space domain of the Universe due to the narrowing of the energy-field region. That is, here we are dealing with a universe where the baryonic matter inside the universe is stable and does not move anywhere in contrast to what the Big Bang model supposedly predicts. So, the Γ-equation highlights the steady state Universe.

7. Discussion

The aim of this investigation was to provide a reliable way for estimating cosmological distances. In our analysis, we started with the Space idealization assuming homogeneity and isotropy of the space; the so-called Copernican Principle was supposed to be valid. Isotropy implies absence of allocated directions (top, bottom and others), thereby

postulating independence of the properties of bodies moving by inertia from the direction of their motion. Complete isotropy is inherent only in vacuum, as anisotropy in the distribution of the binding forces characterizes the structure of real bodies. They split in some directions better than in others if we observe the Universe in grid cells of 50-100 MpC in dimensions. In the same way, complete homogeneity, characteristic only of an abstract Euclidean space, is an idealization. The real space of material systems is inhomogeneous, as it differs in the metric and in the values of curvature, depending on the distribution of gravitating forces.

More often than not, numerous anomalies and paradoxes in cosmology suggest that in the context of Universe dynamics it is prudent for cosmologists to consider the average energy density scale rejecting thereby the space non-homogeneity while retaining the isotropy assumption. However, taking into account our postulate of the gravitational transition, which leads to the growth of space, the homogeneity of energy in space, in contrast, will thus supposedly manifest itself, demonstrating a decrease in energy density with the development of growing phenomena in the visible hemisphere. This speculative postulate, in spite of violation in reality the homogeneity assumption, may lead to correct understanding of space and matter dynamics in the depths of space if a distance to the observed extragalactic object is truly estimated by relying on the light, which was obviously emitted at some point in the past. If we also include the principle of a gravitational transition of energy-field into quantum vacuum and baryonic matter, we believe that we can arrive at a coherent picture of the Universe.

Testing a particular theory, the researcher constructs a hypothesis based on the verifiable facts or previously established theories and examines the obtained data in relation to this knowledge base. To test the gravitational transition assertion objectively, it is necessary to obtain valid data. Still, it is debatable whether available data is an objective basis for verifying the replacement of events on time line by the energy density scale parameter values instead. Referring to the doctrine of Ernst Mach's economy of thought, the kind of math we use is not

important, but how the math predicts the reality is highly relevant. Guided by this premise, we confirmed the validity of employing the average density of energy as a parameter for describing the events in space.

In the context described above, when attempting to verify the correctness of a newly developed theory, a researcher should also take into account the reliability of the data used. In some cases, the theory can be verified by examining it through its own prism—a common strategy when observing the reality. This is not the case here, because the reliability of the data records reported by NED is not in doubt. On the other hand, if there were no high correlations between known methods for calculating distances, e.g. between the modulus or the alternative theory of Noble F., and if there was a clear degree of contradiction with respect to the Hubble's law, a comparative analysis of average density energy scale μ will not be worth the efforts—it will end where it started. The only objection that really matters is that we interpreted the data on the basis of the energy density scale μ using the hypothesis of gravitational transition of the energy-field into quantum vacuum and baryonic matter while the average density μ decreases with the evolution of the Universe. The transition hypothesis cannot be adequately confirmed without accepting the validity of the gravitational transition of energy-field on the basis observations. It is also clear that we are not in the position to provide evidence in support of this assertion.

8. Concluding Remarks

In this study, we presented a speculative equation describing the space and matter composition at the point of emergence from energy-field and as it continues to emerge. Calibrating the equation in accordance with the current mass-energy composition of the Universe allowed us to reach some speculative conclusions with regard to the energy dynamics in the Universe. We suggested treating the Big Bang as a sudden occurrence of freezing gravitational energy, or any other known or unknown type of energy, releasing latent heat. While this was a plausible line of reasoning, the math that can describe this process allowed us to explain the current composition of the Universe.

None of our speculations presented here fundamentally contradicts the latest views on the composition of the Universe in terms of the percentages of quantum vacuum and baryonic matter in proportion to the energy-field. Specifically, contradictions are avoided due to the calibration and by imposing the curvature relationship. Obviously, we eliminated the mathematical impossibility of Big Bang singularity problem of cosmic growth of the geometry from an alleged singularity $r \approx 0$. Instead, we focused on a series of holes/bobbles, represented as hypermanifolds $\mathcal{S}^3$ of radius $0 \le r \le 1$ enclosing the $\mathcal{R}^4$ hyper-globe by adopting radius of space curvature equal to 1. The latter eliminated any ambiguity in the outcomes pertaining to the quantum vacuum and baryonic matter fractions in proportion to the energy-field in case that the grid incorporated gravitational constant G and speed of light c into potential energy measurements, i.e., the case when the grid guarantees the correct output irrespective of the values adopted for G and c.

We were interested in the composition of quantum vacuum, baryonic matter and energy-field, wherever these three components might be in reality. Subsuming the constant G and speed of light c under the energy density parameter μ also resulted in our calculation becoming transparent to the curvature of the space. That was the motivation behind the choice of curvature $\text{const} = 1$. Our speculative equation required fine-tuning or calibration of the so-called Λ-parameter of a speculative space-energy gravitational transition level, as well as the λ-parameter characterizing a modified potential energy-field. This allowed the optimal values to be determined, with respect to achieving the best tuning effect posited by the Planck Mission. Thus, the search for the roots of the equation depending on the average energy of density μ can have some predictive power, since the relative location of the root values in the current μ is almost 100% consistent with the latest Planck Mission Statement about the composition of space and matter in the Universe.

The next important assumption pertained to the energy density parameter μ of the emerging space and matter, to which we referred as an energy density. While acknowledging that the explanation offered for the NED data analysis findings requires more convincing arguments of equivalence of energy and space, we proceeded with our analyses by assuming that the energy density was aligned with the *"normal density"* of matter. The concept of density allowed us to interpret, as well as predict, the dynamics and *"quasi-velocity"* of the formation of a hole or a globe within space. It was also possible to make assertions that essentially coincide with the NASA statement that, in the past, the manifold expanded more slowly than it does presently. As our manifold implies, only a tiny globe of quantum vacuum solves the equation at the higher end of the energy density scale. At this extreme end of the density scale, the manifold comprised solely of energy-field, i.e., when the time $t \leq 0$ since the baryonic matter radius suggested almost a zero solution. At the opposite (lower) extreme of the scale, approaching the critical value, in contrast to the baryonic matter, the quantum vacuum will allegedly start to diminish.

APPENDIX. ***The energy density scale effects***

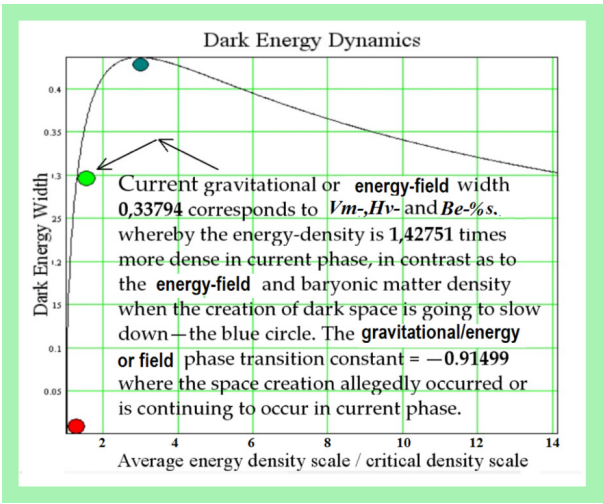

Figure 6: Shows the dynamics of energy-field as a function of density.

The scale of energy density on the x-axis extends from its critical ratio=1 and will continue to reflect the energy-field width as it shifts to the right. If one moves in the opposite direction (to the left), using the analogy implied by the proposed scale, the Figure 6 shows that the formation of quantum vacuum or matter precedes, cf. Carroll (2007), that of baryonic matter because the gap between the two forms increases. On the y-axis, when the inverse stereographical distance $r_1 - r_0 = 2 \cdot \left[\frac{\rho_1}{1+\rho_1^2} - \frac{\rho_0}{1+\rho_0^2} \right]$ reaches some point, it will stop increasing, thus closing the aforementioned gap. The reduction, as indicated in Figure 6, will be most pronounced in the energy density in vicinity of 1, where the red circle indicates the end of the evolution of the manifold—the moment of reaching the critical density κ. Thus, as indicated by the blue circle, at the much later stages of evolution, the gap between the baryonic matter and the quantum vacuum starts to close. The state of the manifold at the current stage—denoted by the green circle—is particularly relevant here, as it indicates the present state of the manifold that has already passed the turnaround point. When the gap started closing, the energy density was about three times greater than that at the present state.

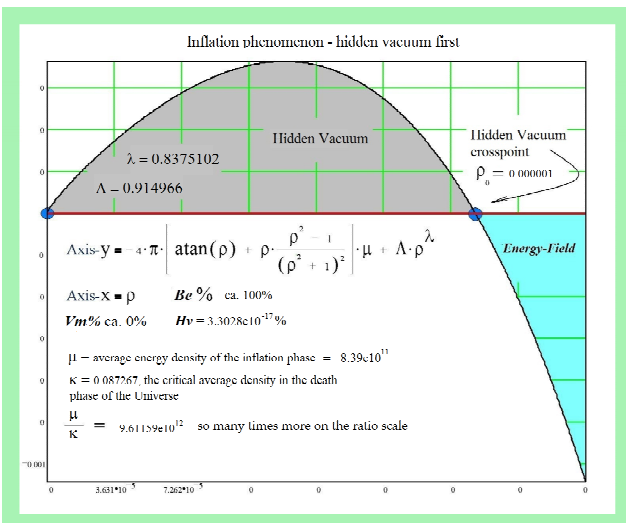

Figure 7: Depicts the case of energy density exceeding a critical value $\kappa \approx 0.087267$ by more than $\approx 9.6115916 \cdot 10^{12}$ times. Quantum vacuum size $\rho_0 \approx 0.000001$

Based on the zero solution $\rho_s \approx 0 > 0$ of the equation, while moving to the right along the x-axis, the speculation states that a positive root $\rho_0 > 0$ can be interpreted as a creation of a small lump of quantum vacuum. We can paraphrase this statement, positing that the quantum vacuum was created first. As it preceded the baryonic matter creation—the inflation Bang of the Big Bang resulted in the emergence of the quantum vacuum only.

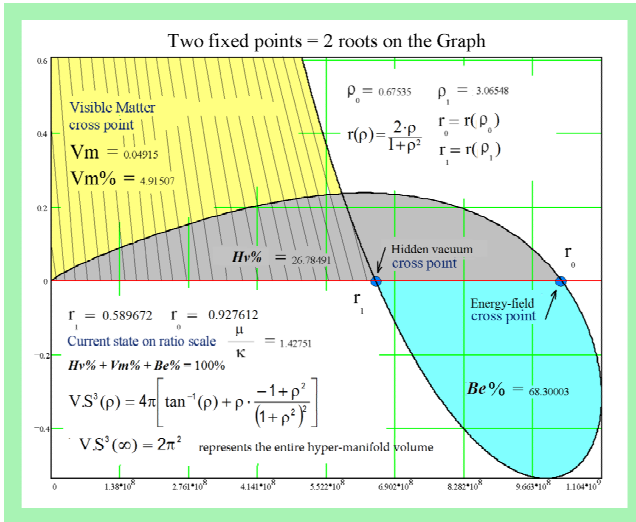

Figure 8: Two roots on opposite poles of S^3 geometry/bubble

The graphical illustration provided in Figure 8, denoting the link between the S^3 manifold and its stereographical projection into Euclidian topology E^3 inflated by quantum vacuum and baryonic matter with regard to energy-field, is the foundation for the study of the essence of all of our Speculations. On the x-axis, the radius r is given by an inverse stereographic mapping $r = \dfrac{2\rho}{1+\rho^2}$ while the y-axis corresponds to

$$\Gamma(\mu,\rho) = -4\pi \cdot \left[\tan^{-1}(\rho) + \rho \cdot \frac{-1+\rho^2}{(1+\rho^2)^2} \right] \cdot \mu + \Lambda \cdot \rho^{\lambda}.$$

The interval $[0 \le \rho \le 1]$ in r-coordinates corresponds to $[0 \le r \le 1]$, whereby the coordinate $r \to 0$ when moving further from 1 corresponds to $\rho \to \infty$. Thus, in the r-coordinate system used in Figure 8, presence of *double curves* on the x/y-axis for $\Gamma(\mu,\rho)$ makes sense.

Two roots (ρ_0, ρ_1) at which the formation of space and matter allegedly occurs solve the equation $\Gamma(\mu, \rho) = 0$. Hence, it can be seen that the graph shown in Figure 8 corresponds to the energy density $\mu = 0.12457$ supposedly representing the current state of the manifold S^3. While passing through the area highlighted in gray, we move r_0 from zero point $0 \to r_0$. In the ρ coordinate system increasing the ρ_0 upward: $0 \to \rho_0$, we are moving along the positive portion of $\Gamma(\mu, \rho)$, which corresponds to 26.8% of quantum vacuum in the Universe composition. Positive $\Gamma(\mu, \rho)$ values indicate the region in the manifold S^3 where the alleged formation of quantum vacuum and baryonic matter already occurred. Similarly, entering the region $\Gamma(\mu, \rho)$ denoting negative values (depicted in blue), we move through the energy-field, which accounts for about 68.3% of the total energy, and is sufficient for further evolution of the manifold. Reaching the radius r_1, we enter the region of baryonic matter, contributing about 4.9% to the Universe composition and moving away from $\rho_1 \le \rho \to \infty$. As depicted in Figure 8, at the radius r_1 and beyond, baryonic matter cannot be in contact with the energy-field in the coordinate system $\rho \in (0, \rho_1)$. However, as it can be seen, it is superimposed on the quantum vacuum at $0 \le r_1$. In conclusion, the scenario depicted in this Figure 8 should be understood as an attempt to visualize the current state in calibrating of the Universe according to the latest data yielded by the Planck Mission measurements.[ii]

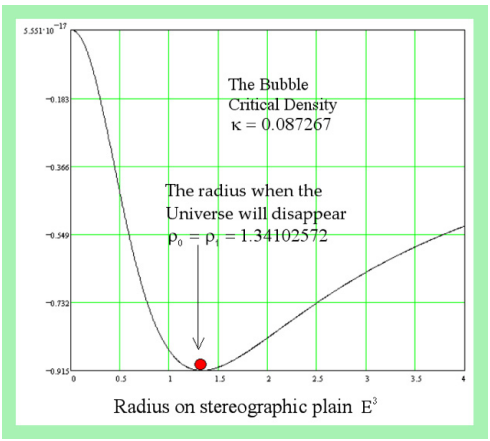

Figure 9: The potential energy governed by the radius starting at point 0.

The case presented by the graph shows on the x-axis in the respective coordinate system ρ our speculative Γ-equation of space and matter creation allowed only a single root, $\rho_0 = \rho_1$. This is the *moment* after which the evolution of the manifold supposedly ceases, since the formation of the new space and matter will terminate upon reaching the critical density κ. At this last *energy-moment*, when the radius $\rho_0 = \rho_1 = 1.34102572$, as indicated by the solution of our **Γ**-equation, the energy density in the manifold will be critical, $\kappa \approx 0.087267$. The manifold in its current state is characterized by density $\mu = 0.12457$, which is, as already pointed above, 1.42751 times greater than the critical density κ at the scale with regard to the critical density starting point. The values of the critical potential energy $-\frac{V.\mathcal{S}^3(\rho)}{\rho^\lambda}\kappa$ are depicted on the y-axis in Figure 9. In this graph, $V.S^3(\rho)$, equal to the volume of a manifold $\mathcal{S}^3(\rho)$ of radius ρ, is multiplied be the critical density κ at which the potential energy reaches its minimum with respect to the critical condition—i.e., the level when only a single root of the **Γ**-equation exists.

Note that the manifold given by Γ-equation, in contrast to that usually adopted does not contain the time scale coordinate. Instead, we used the energy density parameter μ, which declines from very high values that are $96{,}115 \cdot 10^{11}$ times greater than κ. Then we attempt to shift the density towards the critical value $\kappa \approx 0.087267$. Replacing the evolution of the manifold given by **Γ**-equation by the energy density μ parameter is an exercise, due to the scale of *densities*, where declining values replicate the dynamics of space and matter creation within the manifold. Our exercise indicates that the density μ declines towards the current mass-energy composition; it accounts for the μ value pertaining to the current composition, which is at least 1.42751 times denser than $\kappa \approx 0.087267$.

REFERENCES

1. Abbott L., 1988, The Mystery of the Cosmological Constant, Scientific American, vol. 258, no. 5, pp. 106–113. JSTOR, www.jstor.org/stable/24989092 , last visited 2018.06.23.
2. Ade P.A.R., Aghanim N., Armitage-Caplan, C., et al., 2013, Planck Collaboration, 22 March. Planck 2013 results. I. [iii]
3. Arp H., 1966, "Atlas of Pecular Galaxies. "Mount Wilson and Palomar Observatories Carnegie Institution of Washington California Institute of Technology," Published by the California Institute of Technology Pasadena, California 91109.
4. Bradley C.W., Ostlie D.A., 2007, An Introduction to Modern Astrophysics, 2nd ed., Pearson Education, Inc.: Edinburgh Gate, Harlov, 2007-1278.
5. Brzeski J.G., 2007, Expansion of the Universe — Mistake of Edwin Hubble? Cosmological redshift and related electromagnetic phenomena in static Lobachevskian (hyperbolic) Universe. Acta Physica Polonica B, 6, 1501–1520.
6. Caldwell, R.R, Komp W, Parker L., Vanzella D.A.T., A Sudden Gravitational Transition, arXiv:astro-ph/0507622v2 11 Aug 2005.
7. Carroll, S., 2007, The Teaching Company, Dark Matter, Energy-field: The Dark Side of the Universe, Guidebook Part 2, page 46. [iv]
8. Clavin W., 2015, Planck Mission Explores the History of Our Universe. Jet Propulsion Laboratory, Pasadena, California, 818-354-4673.
9. Copeland E.J., Sami, M., Tsujikawa S., 2006, Dynamics of Energy-field. Int. J. Mod. Phys. D, 15, 1753. doi: 10.1142/S021827180600942X.
10. Czerny B. et al., 2018, Astronomical Distance Determination in the Space Age: Secondary Distance Indicators, Space Science Reviews, 214:32.
11. Einstein, A., 2016, The Possibility of a "Finite" and yet "Unbounded" Universe. Chapter 31, Excerpt from: "Relativity", Ang Chew Hoe, iBooks.
12. Francis M., 2013, First Planck results: the Universe is still Weird and Interesting. Ars Technica 21 March.
13. Gradenwitz P., 2018, Analysis of the Expansion of Space and a Theory of the Big Implosion. Journal of High Energy Physics, Gravitation and Cosmology, **2018**, 4, 31-47.
14. Gupta R.P., 2018, Static and Dynamic Components of the Redshift. International Journal of Astronomy and Astrophysics, 8, 219-229. https://doi.org/10.4236/ijaa.2018.83016
15. Guth, A.H.,1997, The Inflationary Universe: The Quest for a New Theory of Cosmic Origins, Basic Books, New York, p. 358. ISBN 0201149427, 9780201149425
16. Jones M.H., Lambourne, R.J., 2004, An Introduction to Galaxies and Cosmology, Cambridge Univ. Press: Cambridge, UK, p.244. ISBN 978-0-521-83738-5.
17. Keel W.C., 2007, The Road to Galaxy Formation, 2nd ed., Springer-Praxis, Chichester, UK, ISBN 978-3-540-72534-3, p.2.
18. Lerner E.J., 2018, Observations contradict galaxy size and surface brightness predictions that are based on the expanding universe hypothesis. MNRAS 477, 3185–3196, doi:10.1093/mnras/sty728, Advance Access publication, March 21.
19. Lerner E.J., Falomo, R., Scarpa, R., 2014, Surface Brightness of Galaxies from the Local Universe to z ~ 5. Int. J. Mod. Phys. D, 23, Article ID: 1450058 [21 pages], DOI: 10.1142/S0218271814500588.
20. Linde, A.D. 1983a, Chaotic Inflation, Physics Letters, 129B, 3, 177-181. 1984b, Раздувающаяся Вселенная, Успехи Физических Наук, Том 144, вып. 2, 1984 г., Октябрь, in Russian.

21. Milgrom M., 1983, A modification of the Newtonian dynamics as a possible alternative to the quantum mass hypothesis, Astrophysical Journal, 270: 365вЂ“ 370, Bibcode:1983ApJ...270..365M, doi:10.1086/161130
22. Mullat J.E., 1995, a) Mathematical Social Sciences 30, pp. 195-205, https://www.sciencedirect.com/science/article/abs/pii/016548969500780P; 1971, b) On a certain maximum principle for certain set-valued functions. *Tr. of Tall. Polit. Inst, Ser. A, 313*, 37-44, (in Russian).
23. Murphy D.M., Koop T.,2005, Review of the vapor pressures of ice and super-cooled water for atmospheric applications. Q. J. R. Meteorol. Soc., 131, 1539–1565. doi:10.1256/qj.04.94.
24. Noble, Forrest W. & Timothy M. Cooper, 2014, "An Alternative Universe-Scale Analytic Metrology and Related Cosmological Model: An Analysis of Type 1a Supernovae Data With Newly Proposed Distance and Brightness Equilibriums Which, if Valid, Would Eliminate the Need for Changing Expansion Rates of the Universe vis-à-vis Energy-field." Appl. Physics Research, Vol. 6, No. 1, pp. 47–67.
25. Ostricker J.P., Peebles P.J.E., 1973, A numerical Study of the Stability of Flattened Galaxies: or can Cold Galaxies Survive? The Astronomical Journal, 186, 467.
26. Perlmutter S. et al., 1999, Measurement of Ω and Λ from 42 high-redshift supernovae. Astrophys. J., 517, 565–586.
27. Pfaltz J.L., 2015, The Role of continuous Process in cognitive Development. Math. Appl. 4, 129-152, DOI: 10.13164/ma.2015.11.
28. Riess A.G. et al., 1998, Observational evidence from supernovae for an accelerating Universe and a cosmological constant. Astron. J., 116, 1009-1038.
29. Rubin V.C., Ford W.K., Jr., 1970, Rotation of the Andromeda Nebula from a Spectroscopic, Survey of Emission Regions. The Astrophysical Journal, 159, 379–403. Bibcode: 1970 ApJ...159..379R. doi:10.1086/150317.
30. Steer I., et al., 2017, Redshift-Independent Distance in the NASA/IPAC Extragalactic Database: Methodology, Content and use of NED-D. The Astronomical Journal 153, 37–57.
31. Tenkanen T., 2019, Dark Matter from Scalar Field Fluctuations. Phys. Rev. Lett..123.
32. Trimble, V., 1987, Existence and nature of dark matter in the Universe. Annual Review of Astronomy and Astrophysics, 25, 425–472. Bibcode:1987ARA&A..25..425T, doi:10.1146/annurev.aa.25.090187.002233
33. Zeldovich, Y.B., Einasto, J., Shandarin, S.F., 1982, Giant voids in the Universe. Nature, 300, 407–413. doi:10.1038/300407a0.
34. Zwicky F., 1933, Die Rotverschiebung von extragalaktischen Nebeln. Helvetica Physica Acta, 6, 110–127.
35. Скляренко, Е.Г., 2008, Курс лекций по классической дифференциальной геометрии, МГУ, Кафедра высшей геометрии и топологии, стр. 32.

---

i Scientific Background on the Nobel Prize in Physics, **2011**. The accelerating universe. The Royal Swedish Academy of Sciences has as its aim to promote the sciences and strengthen their influence in society

ii Planck captures a portrait of the young Universe, revealing the earliest light. University of Cambridge (March **2013**), Retrieved 21 March 2013.

iii This was recognized early on by physicists and astronomers working in cosmology in the 1930s. The earliest Layman publication describing the details of this correspondence is Eddington, Arthur (**1933**). The Expanding Universe: Astronomy's 'Great Debate', 1900–1931.

Cambridge University Press. (Reprint: ISBN 978-0-521-34976-5). Overview of products and scientific results – Table 9. Astronomy and Astrophysics, 1303, 5062. arXiv:1303.5062. Bibcode:2014A&A...571A...1P. doi:10.1051/0004-6361/201321529.

[iv] "...dark matter: An invisible, essentially collision-less component of matter that makes up about 25 percent of the energy density of the universe... it's a different kind of particle...something not yet observed in the laboratory..."

- While philosophy and physics may seem like polar opposites, they regularly address similar questions. Recently, physicists have revisited a modern philosophical topic with origins dating back over a century ago: the unreality of time. What if the passage of time were merely an illusion? Can a world without time make sense?
- While a world without the familiar passage of time may seem far-fetched, several renowned physicists, including string theory pioneer Ed Whitten and theorist Brian Greene, have recently embraced such an idea. A timeless reality may help reconcile the differences between quantum mechanics and relativity, but how can we make sense of such a world? If physics does indeed suggest that the flow of time is illusory, then philosophy may be able to shed light on such a strange notion.
- British philosopher J.M.E. McTaggart advanced this idea in **1908** in his paper titled "The Unreality of Time: http://en.wikisource.org/wiki/The_Unreality_of_Time," last visited 17.07.2017. Philosophers widely consider his paper to be one of the most influential early examinations of this possibility. Looking through McTaggart's philosophical lens, a reality without time becomes a little more intuitive and, in principle, possible.

A Tale of Two Times

- Several interpretations of McTaggart's argument against the reality of time have been put forth. The author's argument starts with a distinction about ordering events in time. The "A" series and "B" series of time form an integral part of McTaggart's argument, which is explicated below by using a historical event as an example.
- On July 20, **1969**, Apollo 11 became the first manned spacecraft to land on the Moon. For the purpose of this discussion, consider this event to represent an event during the present. Several days in the past (July 16), Apollo 11 lifted off the ground. Additionally, several days in the future, all of the mission astronauts will land back on Earth, safe and sound. Classifying an event as "several days prior" or "several days in the future" fits into the "A" series. With respect to the Moon landing, some events (e.g., Lincoln's assassination) are in the distant past, while others are in the distant future (e.g., the inauguration of President Obama), with numerous other events occurring somewhere in between.
- Under the "A" series, events flow from one classification (*i.e.,* past, present and future) to another. On July 16th, the Moon landing would have the property of being in the future. The instant the Apollo 11 landed on the Moon, that event would be deemed as occurring in the present. After this moment, its classification changes to the past.
- The "B" series, however, does not classify events on this scale ranging from the distant past to the distant future. Instead, the "B" series orders events based on their relationship to other events. Under this ordering, Lincoln's assassination occurs *before* the Moon landing, and Obama's inauguration occurs *after* the Moon landing. This relational ordering seems to capture a different way of looking at time.

Two Times, One Contradiction

- Having made this distinction, McTaggart additionally argues that a fundamental series of time requires a change to take place. Under the "B" series, the way these events are ordered never changes. Obama's inauguration, for instance, will never change properties and occur before the Moon landing and vice versa. These relational properties are simply immutable.
- On the other hand, the "A" series does embody the change that we might expect from the flow of time. All events first have the property of being in the future, before becoming current events unfolding in the present. Afterwards, they drift into the past. Under the "A" series, time does have an objective flow, and true change does take place. In McTaggart's view (which is perhaps held by many others), this change is a necessary aspect of time.
- But herein lies the contradiction. If these events do change in this sense, they will have contradictory properties. McTaggart argues that an event cannot be simultaneously in the past, in the present, and in the future. As these properties are incompatible, the "A" series leads to a contradiction. Consequently, time, which requires change, does not truly exist. Welcome to the timeless reality!

Wait a Minute…

- Certainly, many philosophers and physicists still believe in the reality of time and have objected to McTaggart's argument. A number of fascinating caveats and counterexamples can be found elsewhere, such as http://plato.stanford.edu/entries/mctaggart/#UnrTim, last visited 17.07.2017. Nonetheless, McTaggart's work has influenced the approach to time that a number of philosophers have taken, some of whom were inspired by his work and have incorporated physics into their arguments.
- For instance, when Albert Einstein introduced the notion of special relativity, he seriously disrupted our "folk" conception of the flow of time. In special relativity, there is no absolute simultaneity of events. In one reference frame, two events may appear to take place simultaneously. An observer on a speeding rocket ship, however, may observe one event happening before the other. Neither observer is "right" in this situation; this is simply the weirdness that special relativity entails.
- Consequently, many philosophers have used special relativity as evidence refuting the presence of the "A" series of time. If absolute simultaneity does not exist, a statement that one event is "in the present" makes no sense. There is no absolute present that pervades the Universe under special relativity.
- Nonetheless, McTaggart's argument may help us better understand strange physics at the intersection of quantum mechanics and general relativity. In an attempt to reconcile these two theories, some well-known physicists have developed theories of quantum gravity implying that the world lacks time in a fundamental way.
- Brad Monton, a philosopher of physics at the University of Colorado Boulder, recently published a paper comparing McTaggart's philosophy with prominent theories in physics, including quantum gravity (http://philsci-archive.pitt.edu/4615, last visited 17.07.2017). During an interview, We asked him how some of the "timeless" ideas in quantum gravity compared to McTaggart's arguments.

  "They're on par with the radicalness," he said. "There's a lot of radicalness."

- Monton cautioned, however, that quantum gravity does not imply the absence of time that McTaggart may have had in mind. Physicist John Wheeler, as Monton notes, has postulated that time may not be a fundamental aspect of reality. However, this argument applies to extremely small distance scales only.
- Although some of these ideas pertaining to quantum gravity may be radical, several renowned physicists are seriously considering a reality without time at its core. If a quantum gravity theory that requires a radical conception of time emerges, McTaggart may help us better prepare for this new understanding of our world.
- As Monton writes in his paper: "As long as McTaggart's metaphysics is viable, then the answer to the physicists' queries is 'no' – they are free, from a philosophical perspective at least, to explore theories where time is unreal."
- Many quantum gravity theories remain speculative. Still, it is possible that timelessness may become a prominent feature in physics. In such a case, philosophers of science will hopefully help us wrap our heads around the implications.